Journal of Agricultural Chemistry and Biotechnology

Journal homepage & Available online at: www.jacb.journals.ekb.eg

Exploring the Genetic, Structural, and Computational Insights of Resistance Proteins in Arsenic-Bioremediation *Enterobacter* Strain

Asmaa A. Halema[1]; Heba A. R. Abdelhaleem[2]; A. R. Henawy[3]; Nagwa I. Elarabi[1*]; A. A. Abdelhadi[1] and Dalia S. Ahmed[1]

[1]Genetics Department, Faculty of Agriculture, Cairo University; Giza, 12613, Egypt
[2]College of Biotechnology, Misr University for Science and Technology (MUST); 6(th) October City, Egypt.
[3]Microbiology Department, Faculty of Agriculture, Cairo University, Giza, 12613, Egypt

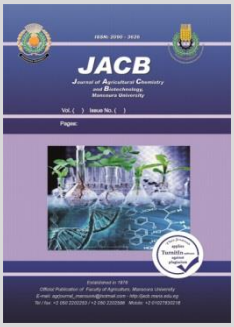

ABSTRACT

Arsenic (As) tops the Agency for Toxic Substances and Disease Registry (ATSDR)'s list of toxic substances, making it a leading cause of severe heavy metal poisoning. This study examined thirty bacterial isolates for arsenic resistance, identifying sixteen strains that could tolerate up to 11,500 ppm of arsenic, a level significantly higher than previously reported. Genetic analysis using rep-PCR profiling revealed significant diversity among these resistant strains. Nine isolates with the highest arsenic tolerance were selected for further study, focusing on arsenic biosorption. Among these, *Enterobacter cloacae* subsp. *cloacae* strain FACU 1 (Ars 9) demonstrated the highest biosorption capacity, removing 85.5% of arsenic from solution, equivalent to 1415 mg/g of biomass. Molecular identification and transmission electron microscopy (TEM) confirmed the existence of arsenic on the cell surface of Ars 9. Furthermore, it was verified that this strain possessed the arsenic resistance genes *Acr3(1), Acr3(2), ArsB* and *ArsC.* These proteins' homology models were produced utilizing SWISS-MODEL and AlphaFold2, and molecular docking was applied to assess their binding affinities for arsenate (AsO4) and arsenite (AsO3). Results indicated that ArsC exhibited a higher affinity for AsO4, suggesting its role in AsO4 reduction. Transport proteins ArsB and Acr3 showed moderate affinities for AsO3, facilitating its efficient efflux. These findings offer valuable insights into bacterial arsenic detoxification mechanisms and highlight the potential of arsenic-resistant strains for bioremediation applications.

Keywords: *Acr3(1), ArsB, ArsC, Enterobacter*, molecular docking

INTRODUCTION

The Earth's crust naturally contains hazardous metalloid arsenic (As) in the form of sulfosalts and insoluble sulfides. Human activities, including the utilize of As in pesticides, herbicides, agrochemicals and medicine, as well as the utilization of poor-quality irrigation water, have significantly contributed to increase As contamination in the environment (Shankar *et al.*, 2014). Natural processes such as volcanic emissions and land erosion can release significant amounts of As into the environment. These actions contribute to As contamination and pose a threat to environmental sustainability (Zhu *et al.*, 2016). These activities alter the composition and functions of soil microbes, induce metabolic and physiological changes in plants, and contaminate surface and groundwater (Zemanova *et al.*, 2021). In addition, As toxicity has an effect on human health and can lead to many symptoms, including skin itching, loss of appetite, weight loss, weakness, skin cancer, lethargy and fatigue. These symptoms can limit physical activities and work capacity. Additionally, As toxicity may lead to chronic respiratory disorders and gastrointestinal problems such as abdominal pain, nausea, anorexia, moderate to severe anemia and enlarged liver and spleen (Banerjee *et al.*, 2011).

Relationship between beneficial soil microbes and harmful metals has become a significant area of global interest due to their potential to improve soil fertility and mitigate metal pollution (Thomas *et al.*, 2020; El-Beltagi *et al.*, 2024). As exists in several forms, for example arsenite (As O3), and arsenate (As O4). Of these, As O3 and As O4 are the most prevalent in the natural environment. Both forms are highly toxic, with As O3 more poisonous. They can inflict diverse types of cellular damage on biological systems (Smedley and Kinniburgh 2002; Achour *et al.*, 2007). Plant roots could absorb both As O4 and As O3. Although they do so in different ways, both types of As inhibit plant metabolism. AsO4, a phosphate analog in chemical reactions, can interfere with phosphate-dependent metabolic processes. Phosphate transport proteins carry it across cellular membranes, causing phosphate supply imbalances. AsO4 can also interfere with phosphorylation reactions by competing with phosphate, leading to the formation of unstable and short-lived AsO4 complexes. AsO3, a dithiol-reactive compound, can bind to and inactivate enzymes containing dithiol cofactors or closely spaced cysteine residues. Exposure to AsO3 often induces the production of reactive oxygen species (ROS), which can subsequently trigger the synthesis of antioxidant metabolites and various antioxidant enzymes (Finnegan and Chen 2012). Furthermore, because As O4 is comparable to phosphate and can block enzymes like kinases, it is harmful to bacteria (Lou *et al.*, 2009). Additionally, AsO4 can enter cells via the same transport mechanisms used for phosphate. This disrupts metabolic processes reliant on phosphorylation, hindering the production of adenosine triphosphate (ATP), an essential

* **Corresponding author.**
E-mail address: nagwa.abdulfattah@agr.cu.edu.eg
DOI: 10.21608/jacb.2024.341775.1098

energy molecule (Shrestha *et al.,* 2008). Arsenite's toxicity stems from its strong binding to sulfhydryl groups (containing sulfur and hydrogen) in proteins. The redox state of cysteine residues present in the active sites of many enzymes is upset by this binding, impairing the enzymes' ability to function. As O3 also interacts with dithiol groups (containing two sulfur atoms) in molecules like glutaredoxin, glutathione and thioredoxin, interfering with cellular redox balance, DNA synthesis and repair processes, and protein folding (Cui and Jing 2019; Kruger *et al.,* 2013). In response to the increasing levels of As in the environment, many microbes have developed mechanisms to detoxify As (Dunivin *et al.,* 2009).

Numerous As-resistant bacteria have been identified that can tolerate high concentrations of As. These microbes hold potential for bioremediation of As-contaminated groundwater. As-resistant bacteria (Gram-negative and Gram-positive) belonging to the genera *Aeromonas*, *Acinetobacter*, *Bacillus*, *Planococcus*, *Exiguobacterium*, *Escherichia* and *Enterobacter* and have been identified. These bacteria play a crucial role in detoxifying As in various environmental conditions (Taran *et al.,* 2019). A *Planococcus* KRPC10YT strain, isolated from an arsenic-contaminated borehole in India, by Chowdhury *et al.,* (2009), can survive in the presence of up to 30 mM As O4 and 20 mM As O3. Shivaji *et al.,* (2005) reported *Bacillus arsenicus*, another arsenic-resistant strain, in the same region. This strain was capable of growing in the existence of 20 mM As O4 and 0.5 mM As O3.

To survive in situations with high levels of arsenic, bacteria have evolved a number of survival methods, including reducing As uptake, methylation and converting As O4 to AsO3. While AsO3 is also toxic, it can be more easily expelled from the cell (Shoham *et al.,* 2021). In addition to the oppositely charged amino groups in bacterial cell walls adsorbing negatively charged As ions, sequestration by various chelation, compartmentalization, immobilization, dissimilatory and exclusion As O4 respiration could be used by bacterial cell (Botes *et al.,* 2007; Tsai *et al.,* 2009). The ars operon, a group of genes involved in As resistance, typically contains *arsRBC* or *arsRDABC* genes. These genes are found on microbe chromosomes or/and plasmids. The proteins produced by these genes, particularly As O4 reductase, enable bacteria to resist and overcome As toxicity (Dunivin *et al.,* 2009). Mechanistically, cytoplasmic As O4 reductase (encoded by *ArsC*) reduces As O4 to As O3, detoxifying As in the contaminated environment. ArsB efflux pump that is membrane bound, which is expressed by the *arsRBC* operon, then expels As O3 from the bacterial cell in the majority of bacteria. By exploiting the membrane potential to expel As O3, the ArsB permease acts as a uniporter. The permease is changed into a more effective ATP-driven As O3 pump that offers improved As O3 resistance when it is linked to ArsA. ArsB family proteins regularly evacuate As O3 and antimonite oxyanions (Meng *et al.,* 2004). Nonetheless, the *arsRDABC* operon encodes the ArsAB pump, which is present in certain bacterial populations (Mukhopadhyay *et al.,* 2002).

As efflux is the primary detoxification mechanism in microorganisms, with six different types of efflux transporters identified: *Acr3*, *ArsB*, *ArsJ*, *ArsK*, *ArsP*, and *MSF1* (Garbinski *et al.,* 2019). Among these, ArsB and Acr3 are highly abundant, even in soils with low As levels, and their presence correlates strongly with As concentrations, making them potential biomarkers for contamination (Castro-Severyn *et al.,* 2021). Protein phylogenetic analysis reveals that ArsB and Acr3 form distinct groups from other As transporters (ArsK, ArsJ, MFS1), indicating functional divergence (Shi *et al.,* 2018). Despite sharing the same function, ArsB and Acr3 evolved independently, showing no sequence similarity (Yang *et al.,* 2015). ArsB belongs to the ion transporters superfamily and is found only in microbes, while Acr3, part of the bile/arsenite/riboflavin transporter (BART) superfamily, is more widespread, occurring in bacteria, fungi and plants (Yang *et al.,* 2015). The distinction between Acr3(1) and Acr3(2), representing multiple copies of the Acr3 gene in some bacteria, is discussed in several studies on As resistance mechanisms in microbes (Fu *et al.,* 2009). Bacteria with multiple Acr3 genes can survive in environments with varying or extreme As concentrations, making them more versatile for bioremediation (Fu *et al.,* 2009).

Molecular docking provides a powerful tool for exploring how heavy metals (HMs) interact with biological molecules (Desai *et al.,* 2024). Docking helps in optimizing the structure of potential chelators by modeling their binding affinity to metals, making it a critical tool in developing drugs or remediation agents for HM poisoning (Aljohani *et al.,* 2021). Docking studies on proteins from HM-resistant bacteria can reveal how these organisms handle metals, aiding in the development of more efficient bioremediation techniques (Tasleem *et al.,* 2023). Due to As toxic effects and the lack of information on microbial arsenic removal, this study focused on isolating bacteria capable of tolerating high As concentrations from industrial pollution sites. The isolated bacterial culture was further evaluated for its maximum As tolerance *in vitro*. In addition, the binding mechanisms of ArsC, ArsB, and Acr3 proteins for As O4 and As O3 detoxification were investigated.

MATERIALS AND METHODS

Chemicals and reagents

Sigma-Aldrich supplied the sodium hydrogen arsenate ($Na_2HAsO_4.7H_2O$) (cat. no. 10048-95-0, USA). The stock solution was prepared as 20%, which was then sterilized using 0.22 µm sterile syringe filters (Millex® PVDF syringe filter, Sigma-Aldrich, cat. no. SLGVR33RB, USA). The stock solution mentioned above was diluted to get the other concentrations.

Samples collection

Industrial wastewater samples were collected from two locations in Egypt: the industrial zone, Borg Al Arab Al Gadida City, Alexandria Governorate (coordinates: 30°50'28.2"N 29°36'22.7"E), and the industrial zone, 10th of Ramadan City, Ash Sharqia Governorate (coordinates: 30°16'36.7"N 31°47'12.8"E). These locations are highly contaminated with HMs, according to multiple researches, i.e., (Elarabi *et al.,* 2023; Halema *et al.,* 2024; Abdelhadi *et al.,* 2024). As concentration in samples was evaluated utilizing atomic absorption spectrophotometer (Buck Model 210 VGP) according to Kunkel and Manahan 1973 and Patnaik 2017). To guarantee accuracy, each measurement was conducted three times.

Isolation of As-resistant bacteria

According to Abdelhadi *et al.,* (2024), industrial effluent samples were employed to isolate As-resistant bacteria. Simply, 0.1 ml of diluted wastewater was sprayed onto Luria-Bertani (LB) plates with increasing concentrations

of $Na_2HAsO_4.7H_2O$ (50, 100, 250, 500, 1000, and 1200 ppm). For five days, the plates were incubated at 30 °C.

Minimum inhibitory concentration (MIC) and maximum tolerance concentration (MTC) evaluation

To calculate the MIC and MTC, selected isolates that were cultured at 1200 ppm were picked utilizing agar plate dilution method as outlined by Malik and Jaiswal (2000) and Afzal *et al.,* (2017). LB agar plates with eight distinct concentrations of $Na_2HAsO_4.7H_2O$ (1500, 3000, 3500, 5000, 6500, 8000, 9500, and 11500 ppm) were prepared using this approach (Dey *et al.*, 2016; Mandal *et al.*, 2022). Following sterilization, selected isolate was added to the plates. The MIC and MTC were calculated using bacterial growth patterns during a 7-day incubation period at 30 °C.

Rep-PCR DNA profiling

BOX, enterobacterial repetitive intergenic consensus (ERIC) and Repetitive extragenic palindromic (Rep) specific primers were utilized for genetic diversity assessments of sixteen As-resistant isolates (Henawy *et al.*, 2023) (Table 1).

Table 1. The primers sequences and annealing

Primer name/Genes	Sequence (5'-3')	Annealing temperature (º C)	Reference
	Rep-PCR DNA profile		
BOXA1R	CTACGGCAAGGCGACGCTGACG	52	(Çepni *et al.,* 2001)
$(GTG)^5$	GTGGTGGTGGTGGTG	52	(Gevers *et al.,* 2001)
ERIC2R	ATG TAAGCTCCTGGGGATTCAC	52	(Versalovic *et al.,* 1994)
MBO REP1	CCGCCGTTGCCGCCGTTGCCGCCG	52	(Genersch and Otten 2003)
16S rRNA gene			
27F	AGAGTTTGATCMTGGCTCAG	58	(Abdelhadi *et al.,* 2016)
1492R	TACGGYTACCTTGTTACGACTT		
	As-resistant genes		
ArsC	GTAATACGCTGGAGATGATCCG TTTTCCTGCTTCATCAACGAC	57–52 ºC, decreasing by 0.5 ºC every cycle for the first ten cycles	(Selvi *et al.,* 2014)
ArsB	GGTGTGGAACATCGTCTGGAAYGCNAC CAGGCCGTACACCACCAGRTACATNCC		(Achour *et al.,* 2007)
Acr3 (1)	GCCATCGGCCTGATCGTNATGATGTAYCC CGGCGATGGCCAGCTCYAAYTTY TT		(Achour *et al.,* 2007)
Acr3 (2)	TGATCTGGGTCATGATCTTCCCVATGMTGVT CGGCCACGGCCAGYTCRAARAARTT		(Achour, 2007)

Standard ambiguity codes are utilized to indicate degenerate nucleotide sites: N for any nucleotide, R for purine, V for A, C, or G, and Y for pyrimidine.

DNA was extracted applying the Simply™ Genomic DNA Isolation Kit (GeneDireX, Inc., Cat. No. SN023-0100, Taiwan), following manufacturers' guidelines. For a 10 µL reaction volume, 50 ng/µL DNA, 2X OnePCR™ master mix (GeneDireX, Inc., Cat. No. MB203-0100, Taiwan), 10 pMOL from each primer, 150 µg of BSA and complete the reaction with nuclease-free water. DNA profiles were examined utilizing the PyElph 1.4 software. The Past software was applied for the similarity and distance index. As well, heatmap was constructed by Origin Pro 2022. Polymorphic Information Content (PIC), Discriminating Power (DP) and Marker Index (MI) were calculated utilizing iMEC program (Amiryousefi *et al.*, 2018).

Bacterial survival percentage under As condition

Bacterial isolate survival and suppression rates were assessed using the Colony-Forming Unit (CFU) assay after 5 days of exposure to high As concentrations. The selected isolates were cultured on LB media, both with and without 9500 ppm of $Na_2HAsO_4.7H_2O$ (the MTC concentration), at 30°C on a shaker at 150 rpm for 5 days. Subsequently, sterilized deionized water was used to perform successive dilutions to 10^{-6}. On free LB solid media, 0.1 ml of the diluted solution was then added. Using the spread plate approach, CFUs of selected isolates were obtained (Elarabi *et al.,* 2023). The isolates with survival percentages more than 50% were nine isolates, which were selected for further experiments.

Determination of As biosorption and its efficiency

The bacterial isolates' rates of As removal were assessed using LB media supplemented with 9500 ppm of $Na_2HAsO_4.7H_2O$. For five days, the suspension of chosen isolates with an OD^{600} value of 1.0 was cultured into 25 ml of LB medium and shaken at 150 rpm per minute at 30 degrees Celsius. For 20 minutes, the treated isolates cultures were centrifuged at 5000×g. Following two dH_2O washes, the collected cells were baked for 48 hours at 80 °C to dry them out. The dry weight of the bacteria was then calculated. Supernatants were exposed to inductively coupled plasma atomic emission spectroscopy (ICP-AES) to evaluate the residual As ion concentration. The As biosorption % and biosorption (mg/g) were computed following the methodology outlined by Pagnucco *et al.,* (2023) and Vijayaraghavan and Yun (2008).

Bacterial identification utilizing the *16S rDNA* gene

DNA was collected employing the Simply™ Genomic DNA Isolation Kit (Cat. No. SN023-0100, GeneDireX, Inc., Taiwan) due to manufacturer's instructions for molecular identification. Universal primers of the *16S rDNA* gene were utilized (Table 1). A 50 µL PCR reaction was prepared containing DNA (50 ng/µL), OnePCR™ master mix (2X) (Cat. No. MB203-0100, GeneDireX, Taiwan), forward and reverse primers (10 pMOL) and completed with dH2O.

TEM analysis

Transmission electron microscopy (TEM) analysis was implemented at the Cairo University Research Park (CURP), Giza, Egypt, to investigate potential structural changes and metal accumulation/adsorption sites in cells exposed to As stress. The highest significant biosorption capacity Enterobacter cloacae subsp. cloacae strain FACU 1 (Ars 9) was chosen for this analysis. The strain was cultured in liquid LB media with 9500 ppm As as a treated group and without As as a control group. TEM was performed on both

As-treated and control bacteria utilizing a Tecnai G20 TEM (FEI, Limeil-Brevannes, France) at 200 kV (Burghardt and Droleskey, 2006). Images were picked utilizing digital CCD camera and processed with Germany Olympus Soft Imaging System's iTEM software.

Isolation of four As genes

Two degenerate primer sets were utilized for the amplification of the arsenical pump membrane gene (*ArsC* and *ArsB*) and As O4 carrier families (*Acr3(1)* and *Acr3(2)*) (Table 1). Denaturation for 5 minutes at 94°C and 40 cycles (denaturation for 60 second at 94°C, annealing for 60 second in accordance with Table 1, extension for 120 second at 72° C) and, as a last step, 5 minutes at 72° C were the PCR procedures. ExoSAP-ITTM PCR Product Cleanup Reagent (Applied Biosystems, Cat. No. 78201, USA) was used to purify the PCR product. To identify the isolated bacteria and investigate their As resistance genes, the purified *16S rDNA* gene and four As resistance genes were sequenced by Macrogen Inc., South Korea. ClustalOmega was utilized to align the *16S rDNA* nucleotide sequences of our isolates and the most closely related ones (Madeira *et al.,* 2019). The sequenced genes were posted to GenBank and then aligned with existing entries using both the NCBI BLAST tool (http://www.ncbi.nlm.nih.gov/BLAST/) and EzBioCloud DB software (https://www.bioiplug.com/). TrimAl version 1.4.rev22 was used to trim the alignment result (Capella-Gutiérrez *et al.,* 2009). Highly similar sequences were picked and aligned with Clustal Omega. A phylogenetic tree of *16S rDNA* was then performed using MEGA 11 with the Maximum Likelihood method (Timura-Nei 3-parameter model). Bootstrapping with 1000 replicates was performed to assess the data's reliability.

Molecular docking

With the use of the ProtParam program (https://web.expasy.org/protparam/), several physical and chemical parameters were calculated from the inferred amino acids of the four As resistance genes (Azimi *et al.,* 2024).

Using the AlphaFold 2 internet webserver (https:// neurosnap .ai/ service/AlphaFold2) and the SWISS-MODEL web server (https://swissmodel.expasy.org), the four protein FASTA sequences were further used in homology modeling to produce a protein model (Schwede *et al.*, 2003; Skolnick *et al.,* 2021). Two As model compounds that have been previously reported were chosen because of their toxic qualities: AsO4 and AsO3, the two forms of As that are most frequently found globally. The three-dimensional structures of arsenate (ART) and arsenite (AST) were retrieved from the Protein Data Bank (PDB) (https://www.rcsb.org/) (Berman *et al.*, 2000). Both of the previously stated proteins underwent extensive protein conformational changes with the use of the CABS-flex 2.0 web server resource (http:// biocomp .chem .uw. edu. pl/ CABS flex2). The computationally effective CABS-flex model was used in place of the widely used method for protein simulation, all-atomic molecular dynamics. According to Jamroz *et al.*, (2014), the CABS-flex simulation methodologies rely on a data methodology based on molecular dynamics modeling.

Using AutoDock Vina (v. 1.2.0), the refined proteins under study were deployed in docking to determine the binding affinity with As models (Eberhardt *et al.*, 2021). The Auto Dock Tool (ADT) was used to optimize and prepare the ligands as ART before docking was done on them. Following the initial setup of the necessary parameters, the ligands were saved in SDF format and the proteins in PDBQT format. Both the ligand and the proteins remained stiff during the whole docking process. The data with the best free binding energy was picked to represent a cluster of results with a positional root-mean-square deviation (RMSD) of less than 1.0. We predicted that ligand-binding affinities would lead to negative Gibbs free energy (G) scores (kcal/mol) utilizing AutoDock Vina scoring method (Morris *et al.*, 2009; Forli *et al.*, 2016). Highest negative binding free energy and associated RMSD values originating from the experimentally discovered binding sites dominated the AutoDock findings rankings. According to the binding energies displayed by Vina, the highest ranked binding free energy always translates into an RMSD value of 0 (Forli *et al.*, 2016). For further examining binding attributes, best-fitting (surface) ligand in posture with lowest binding energy or affinity was drawn and picked.

Statistical analysis

The R package (agricolae) version 1.4.0 (Mendiburu and Yaseen 2020) was applied to conduct one-way analysis of variance (ANOVA) and least significant difference (LSD) tests. GraphPad Prism 8 software was applied for visualization.

RESULTS AND DISCUSSION

Results

Isolation of As resistant bacteria

Firstly, the As concentrations in the collected samples, Borg Al Arab Al Gadida City and the 10th of Ramadan City samples, were measured and recorded as 3.8± 0.11 and 0.16± 0.01 mg/L, respectively. At a $Na_2HAsO_4.7H_2O$ concentration of 1200 ppm, thirty bacterial isolates were picked. Then, MIC and MTC of these isolates were performed. At the concentration of 9500 ppm, there were sixteen isolates that could grow, and we can consider this MTC as shown in Fig. (1). These isolates were coded as AI from 1 to 16. The higher concentrations used up to 11500 ppm, the lower the isolate number obtained. However, the MIC for all isolates was 11500 ppm.

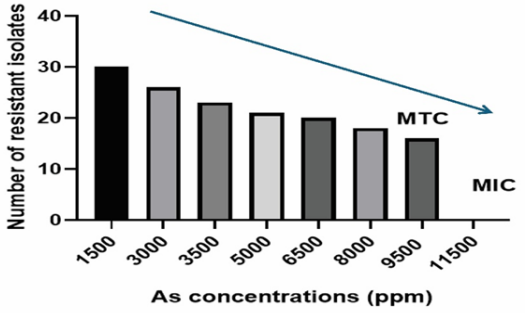

Fig. 1. The number of isolates that can resist As at different concentrations to determine MIC and MTC

Genetic variation analysis utilizing Rep-PCR-DNA profiling

Rep-PCR-DNA profiling assessment was performed utilizing four primers with 16 As-resistant isolates, which can resist until 9500 ppm, in order studying the genetic diversity among the selected strains. Table 2 summarizes the genetic diversity parameters, including total number of amplicon, polymorphic amplicon, unique positive amplicon, percentage

polymorphism, PIC, MI, and DP. In addition, heatmap and cluster analysis based on similarity and distance indices of Dice similarity values of the 16 isolates was indicated in Fig. (2). There were 86 amplicon in all primers, including 22, 24, 21, and 19 amplicon by the independent primers BoxA1R, ERIC2R, $(GTG)^5$, and MBO REP1, respectively. Every primer generated amplicon that were 100% polymorphic. No negative unique amplicon were identified, but the number of positive unique amplicon using primers BoxA1R, ERIC2R, $(GTG)^5$ and MBO REP1 was 3, 4, 1 and 2, respectively. With 24 amplicon amplified, ERIC2R had the most amplicon. The range of PIC values was around 0.33 to 0.37. The MI was between about 0.0043 and 0.0162. In turn, the DP varied from 0.7 to 0.9. Therefore, it is possible that the 16 isolates are distinct isolates.

Table 2. Rep-PCR DNA profiling result

Primer name	Total amplicon	Polymorphic amplicon	Positive unique amplicon	Negative unique amplicon	Polymorphism (%)	PIC	MI	DP
BOXA1R	22	22	3	0	100	0.365449	0.012935	0.838217
ERIC2R	24	24	4	0	100	0.338671	0.004397	0.90072
(GTG)5	21	21	1	0	100	0.374822	0.016211	0.763991
MPO REP1	19	19	2	0	100	0.367638	0.013426	0.828831
Total	86	86	10	0	-	1.44658	0.046969	3.331759
Combined	21.5	21.5	2.5	0	100	0.362922	0.01243	0.847014

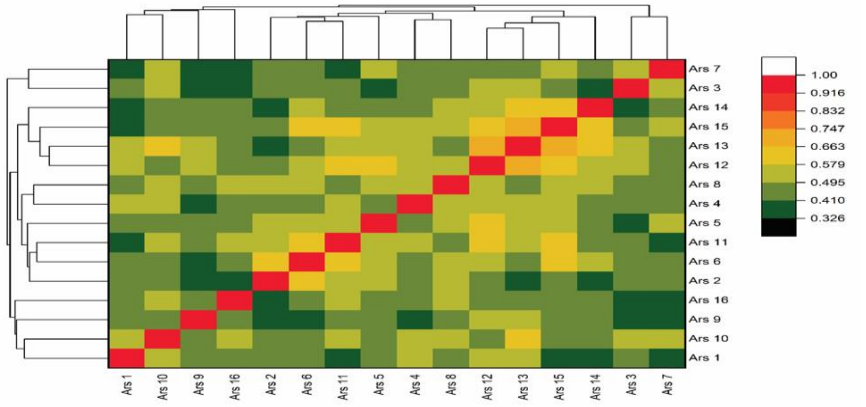

Fig. 2. Heatmap and cluster analysis based on similarity and distance indices of Dice similarity values

Evaluating the As resistance isolates ability

First, among the sixteen isolates, cell viability was measured, and isolates with more than 50% survival percentage were selected when exposed to As supplemented to the media with a 9500 ppm concentration. The number of isolates became nine, which will be measured for their As biosorption and their efficiency of biosorption. However, LSD and one-way ANOVA tests displayed significant differences between these isolates; the highest 5 isolates (Ars 1, Ars 4, Ars 5, Ars 8, and Ars 9) didn't have a significant difference between them and recorded a survival percentage of approximately 92.6%, as shown in Fig. (3A). Furthermore, Ars 9 isolate had the highest significant As biosorption (1415 mg/g) with efficiency (85.5%), as represented in Fig. (3B and 3C).

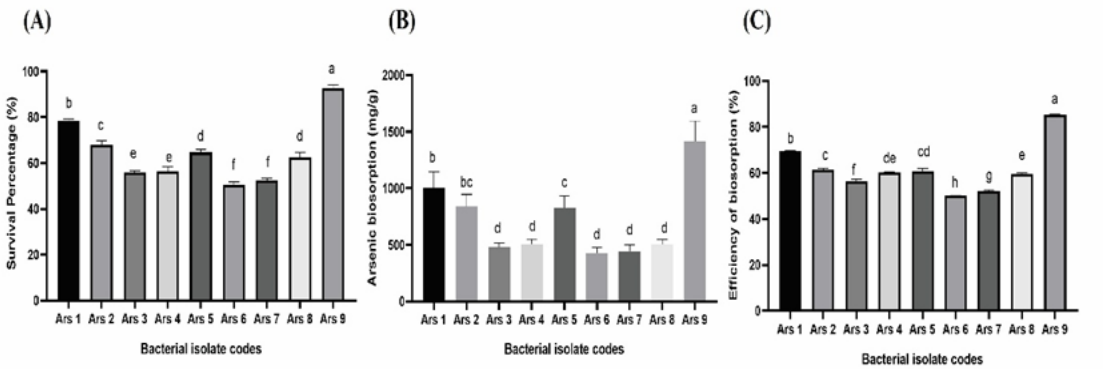

Fig. 3. Assessment the ability of the nine isolates to resist As involved three parameters: (A): the bacterial survival (%); (B): the As biosorption (mg/g) and (C): the efficiency of biosorption (%). ANOVA and LSD tests were evaluated utilizing R package and visualized by GraphPad Prism 8 software

Molecular identification utilizing *16S rDNA* gene

The *16S rDNA* genes (1500 bp) of nine isolates were amplified using PCR and sequenced. *16S rDNA* gene nucleotide sequences were aligned to GenBank databases utilizing BLAST methods. All *16S rDNA* nucleotide sequences of the strains were uploaded in NCBI under the strain code FACU. These include *Enterobacter ludwigii* strain FACU, *Pseudomonas* sp. strain FACU1, *Bacillus*

paramycoides strain FACU1, *Bacillus cereus* strain FACU, *Raoultella planticola* strain FACU1, *Klebsiella pneumoniae* subsp. *ozaenae* strain FACU, *Shigella flexneri* strain FACU2, *Klebsiella quasipneumoniae* subsp. *quasipneumoniae* strain FACU, and *Enterobacter cloacae* subsp. *cloacae* strain FACU1. The percentage similarity of each sequence to existing sequences in the database is presented in Table 3. Between 97.42 and 99.58% of the nine strains were identical. The phylogenetic tree was performed utilizing strains' 16S rDNA sequences, as well as those of their closely related strains and type strains of each genus (Fig. 4).

Table 3. The *16S rDNA* Accession number, the top-hit taxon, similarity %, and bacterial identification

Isolate code	*16S rDNA* Accession number	Top-hit taxon	Similarity (%)	Bacterial identification
Ars 1	MT912693	*Enterobacter ludwigii* strain EN-119	99.54	*Enterobacter ludwigii* strain FACU
Ars 2	MT912695	*Pseudomonas* sp. strain 063	97.42	*Pseudomonas* sp. strain FACU1
Ars 3	MT912696	*Bacillus paramycoides* strain MCCC 1A04098	98.82	*Bacillus paramycoides* strain FACU1
Ars 4	MT912702	*Bacillus cereus* strain ATCC 14579	99.58	*Bacillus cereus* strain FACU
Ars 5	MT912704	*Raoultella planticola* strain DSM 3069	99.25	*Raoultella planticola* strain FACU1
Ars 6	MW599724	*Klebsiella pneumoniae* strain DSM 30104	99.43	*Klebsiella pneumoniae subsp. ozaenae* strain FACU
Ars 7	ON426808	*Shigella flexneri* strain ATCC 29903	99.29	*Shigella flexneri* strain FACU2
Ars 8	MT912633	*Klebsiella quasipneumoniae* strain cjy02	99.53	*Klebsiella quasipneumoniae subsp. quasipneumoniae* strain FACU
Ars 9	MT912689	*Enterobacter cloacae* subsp. cloacae strain FACU	99.54	*Enterobacter cloacae subsp. cloacae* strain FACU1

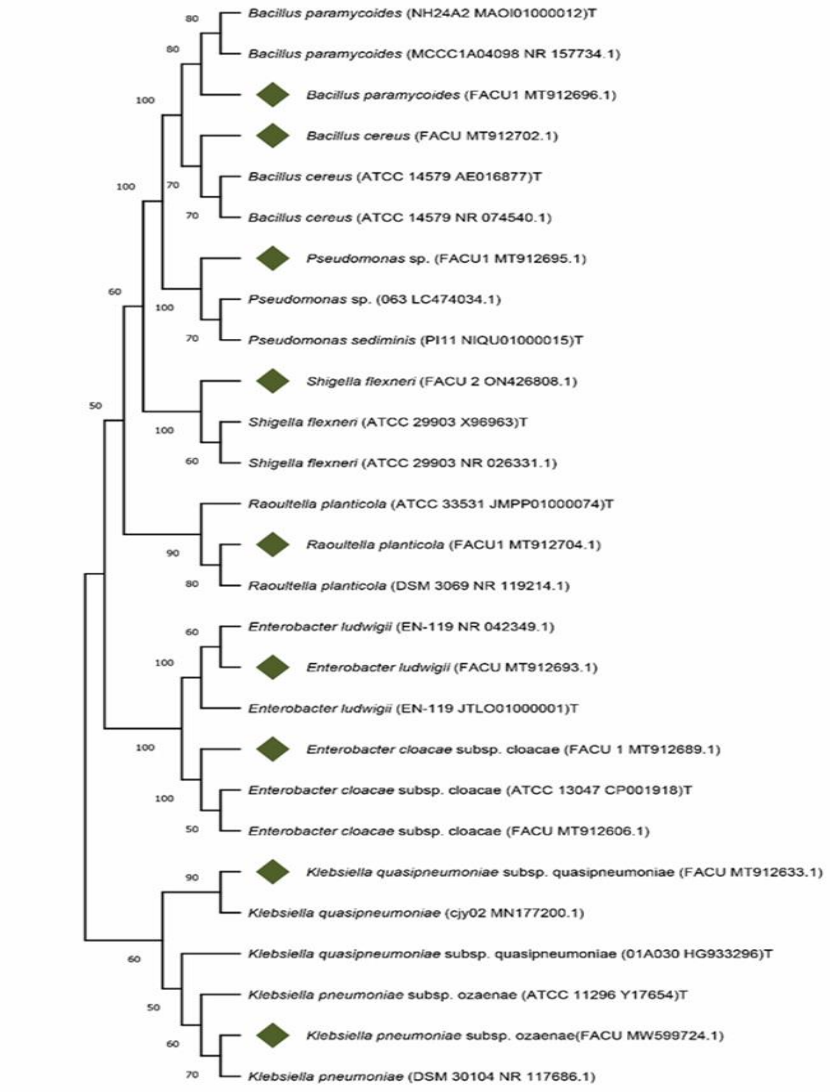

Fig. 4. The nine As-resistant strains phylogenetic tree. Phylogenetic analyses were conducted in MEGA 11, with 1000 bootstrap replicates to assess tree reliability.

Cellular morphological alterations induced by As stress

TEM were utilized to examine how As binds to the surface of *Enterobacter cloacae* subsp. *cloacae* strain FACU 1 (Ars 9). By comparing As-treated cells to untreated cells, we observed changes in cell shape and size, as shown in Fig. (5). The treated cells appeared smaller and had dark spots on their cell walls (Fig. 5B).

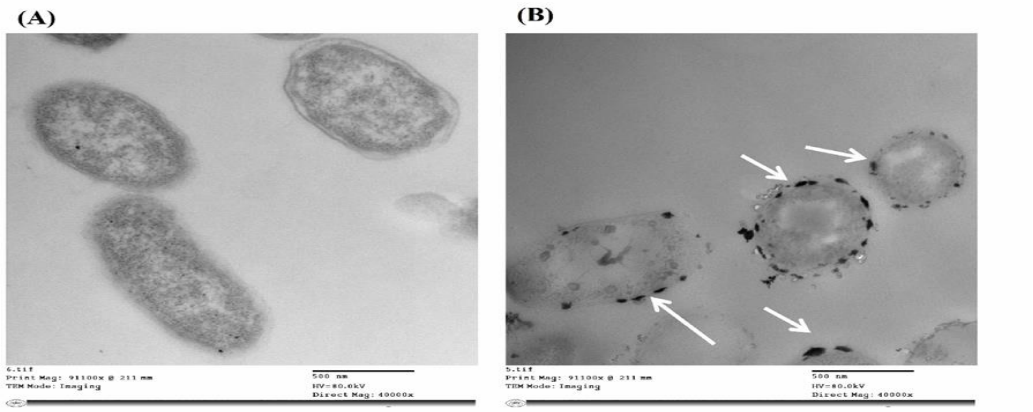

Fig. 5. TEM of the *Enterobacter cloacae* subsp. *cloacae* strain FACU 1 (Ars 9) (A) control without As and (B) with As. Arrows showed the site of the metal adsorption contrasts.

Isolation of four arsenic-resistant genes

The highest significant strain in biosorption capacity (*Enterobacter cloacae* subsp. *cloacae* strain FACU1) was used to isolate four arsenic-resistance genes (*Acr3(1), Acr3(2), ArsB* and *ArsC*) utilizing specific primers (Table 1).

The PCR-produced amplicon sizes were approximately 414, 870, 759, and 732 bp, respectively. Following their purification, these amplicons were sequenced and uploaded to GenBank databases with the corresponding accession numbers PQ434860, PQ424116, PQ434858, and PQ434859.

Protein and ligand preparation for computer analysis

Two model compounds of As, As O4 (ART) and As O3 (AST), were chosen and their three-dimensional structures were recovered from the PDB database as shown in Fig. (6). As indicated in Table 4, the ligand's structural geometry, charge distribution, hydrogen bonding potential, and other key properties were optimized to ensure its accuracy as an ART and AST for docking. Standard parameters were used to build the four proteins in automated mode. The FASTA sequence derived from the deduced amino acids of their genes was used to build these models. As shown in Fig. (6), the SWISS-MODEL workspace offers access to experimental 3D structures that can be utilized to construct simple to complex protein homology models.

Table 4. Chemical properties of model compounds of As with various parameter attributes

Chemical components	(Arsenate) ART	(Arsenite) AST
Formula	As O_4	As O_3
Molecular Weight	138.919	122.92
Type	NON-POLYMER	NON-POLYMER
Isomeric SMILES	[O-][As](=O)([O-])[O-]	[O-][As]([O-])[O-]
Formal Charge	-3	-3
Atom Count	5	4
Bond Count	4	3
Aromatic Bond Count	0	0

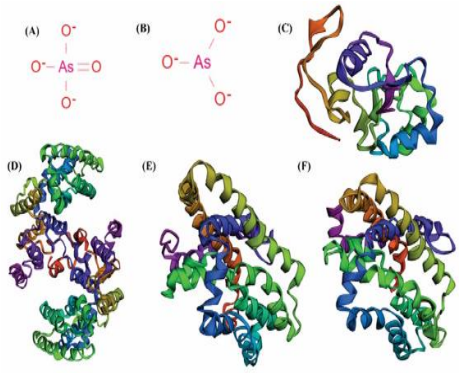

Fig. 6.The three-dimensional structures of the ligands, ART (A) and AST (B), and the studied proteins, ArsC (C), ArsB (D), Acr3(1) (E), and Acr3(2) (F), were predicted by the SWISS-MODEL web server.

The majority of query proteins with clearly defined 3D structures and built-in parameters for structural assessment were the focus of the inquiry, as indicated in Table (5). Moreover, the computation of various physical and chemical parameters for the four studied proteins was performed utilizing the ProtParam tool. Table (5) illustrates the calculated characteristics, which include the molecular weight, theoretical isoelectric point (pI), amount of amino acids, aliphatic index, instability index, estimated half-life and grand average of hydropathicity (GRAVY).

Monomer state with a GMQE value of 0.96 and a sequence identity of 93.43% was used to construct the ArsC model. For every constructed model, several critical parameters were acquired, including Outliers in

Rotamers (0.00%), Ramachandran Favored (99.26%), Bad Bonds (0/1113) and Bad Angles (4/1514). Additionally, the ArsB model was constructed with a GMQE value of 0.94 and a sequence identity of 93.43% in a monomer

form. A few key parameters were acquired for every constructed model, including Outliers in Rotamers (0.00%), Ramachandran Favored (98.26%), unusual Ramachandran results (0.00%), Bad Bonds (0/2250), Bad Angles (12/3077), and MolProbity Score (0.66). Also, at a monomer stage with a GMQE value of 0.88, the Acr3(1) model was constructed with a sequence identity of 84.46%. Several critical parameters were acquired for every constructed model, including unusual Ramachandran results (0.00%), Ramachandran Favored (98.39%), Outliers in Rotamers (0.00%), Bad Bonds (0/1987), Bad Angles (18/2725), and MolProbity Score (0.74). At monomer state with a GMQE value of 0.89, the Acr3(2) model was constructed with sequence identity of 77.78%. Several critical parameters were acquired for every constructed model, including Outliers in Rotamers (0.51%), Ramachandran Favored (97.11%), Outliers in Rotamers (0.00%), Bad Bonds (2/1937), and Bad Angles (16/2652). Regarding the model that was produced from their primary sequences, the protein models show a high degree of accuracy and show no errors in their geometrical coordinates. The built protein models with important properties are shown in Table (5) and Fig. 7 and 8. Moreover, AlphaFold2 helps us to build 3D structures and provides other assessments like predicted local distance difference test (pLDDT) per position, multiple sequence alignment (MSA) coverage, and predicted aligned error (PAE), as shown in Figs. (9, 10 and 11). pLDDT of all proteins is more than 80, which indicates high quality and high certainty of these protein structures. The MSA coverage is mostly strong for the ArsC protein, with high sequence conservation over most of the sequence. The drop-off near the C-terminal end (after position 120) highlights a region with greater variability, possibly indicating species-specific adaptations or non-essential regions of the protein. These insights would be important in understanding the conserved functional domains and variable regions of the ArsC protein across different bacterial species. The MSA sequence coverage of ArsB protein was strong and consistent across most of the query sequence, with high coverage (up to 3000 sequences) across positions 10–250, indicating robust conservation across these regions. Both proteins, Acr3(1) and Acr3(2), have regions of high conservation and some areas where sequence variability or structural flexibility might occur, particularly around position 100 in each case. These dips could represent loop regions, insertions, or deletions in the protein, or possibly regions under less evolutionary pressure to maintain the same structure across species. PAE of the four proteins in Fig. 11 (A, B, C, and D) likely corresponds to different regions of a protein. Lower errors (darker colors) suggest good structural confidence, while areas with higher errors (yellow zones) point to less reliable predictions. ArsC protein has the lowest errors compared to ArsB, Acr3(1), and Acr3(2).

Table 5. Comparative modeling-derived detailed parameters and physical and chemical parameters of the four studied proteins

Parameters / Proteins	ArsC	ArsB	Acr3(1)	Acr3(2)
Score for MolProbity	1.35	0.66	0.74	1.01
Favorite Ramachandran	99.26%	98.26%	98.39%	97.11%
Unusual Ramachandran Results	0.00%	0.00%	0.00%	0.00%
Outliers in Rotamers	0.00%	0.00%	0.00%	0.51%
Bad Bonds	0 / 1113	0 / 2250	0 / 1987	2 / 1937
Bad Angles	4 / 1514	12 / 3077	18/ 2725	16/ 2652
amino acids number	137	289	251	244
Molecular weight	15590.97	30924.05	27400.21	26751.43
Theoretical pI	5.43	9.05	7.82	9.30
Total negatively charged residues number (Asp + Glu)	19	15	9	9
Total positively charged residues number (Arg + Lys)	16	17	10	14
Total atoms number	2207	4493	4001	3889
Estimated half-life	>10 hours	>10 hours	>10 hours	>10 hours
Instability index	46.82	21.57	31.49	36.57
Aliphatic index	95.99	138.82	148.41	143.93
GRAVY	-0.318	1.077	1.151	1.049

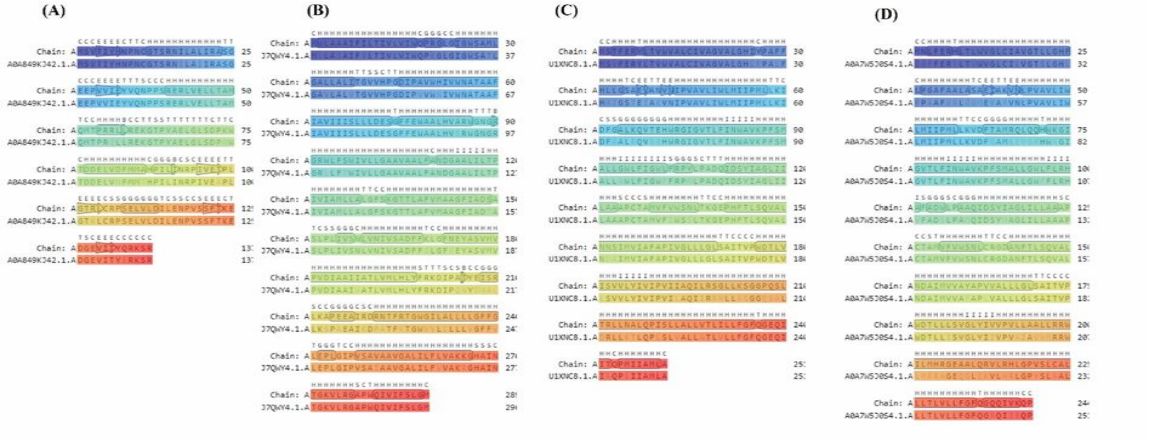

Fig. 7. Query proteins alignment with target protein chains BlastP, ArsC (A), ArsB (B), Acr3(1) (C), and Acr3(2) (D).

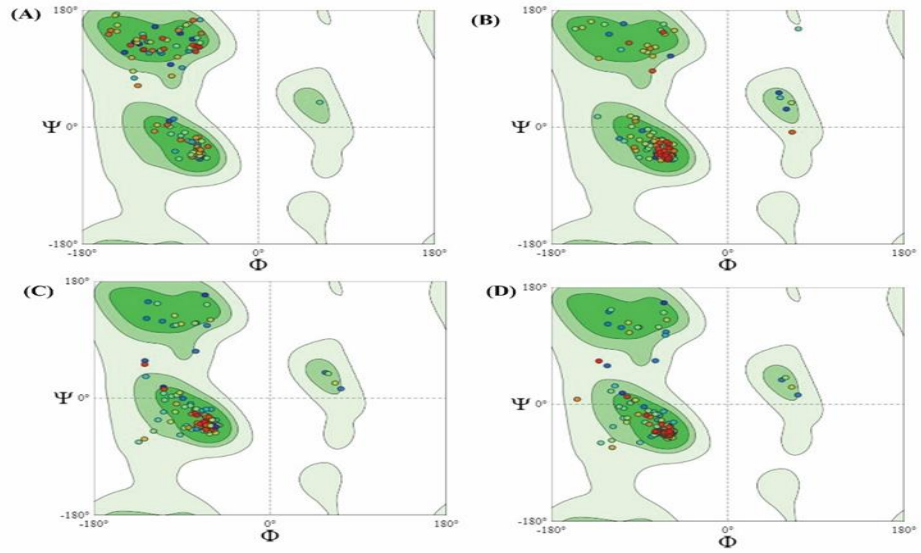

Fig. 8. Ramachandran plot of the protein models, ArsC (A), ArsB (B), Acr3(1) (C), and Acr3(2) (D).

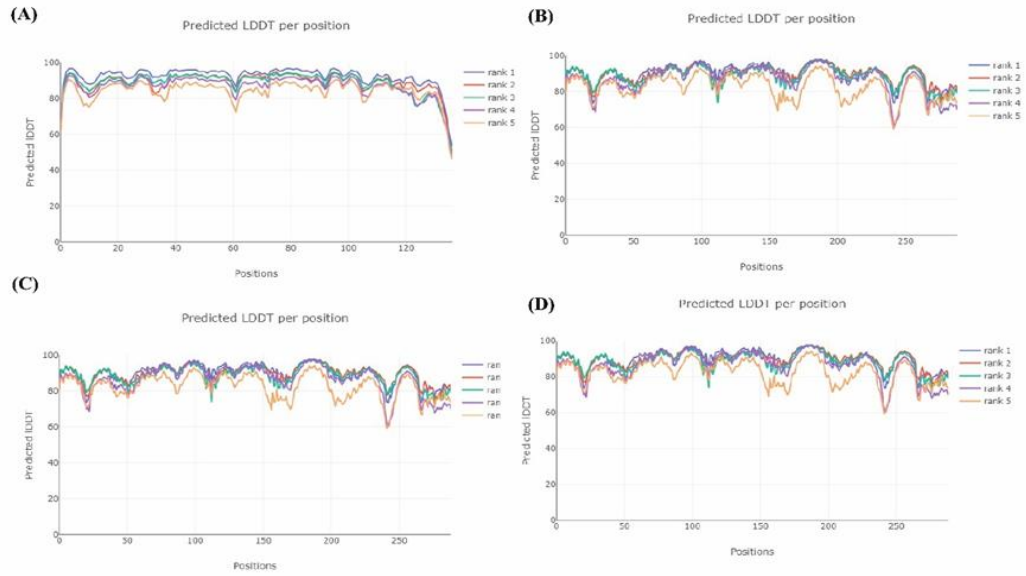

Fig. 9. pLDDT per position of the four proteins (ArsC (A), ArsB (B), Acr3(1) (C) and Acr3(2) (D).

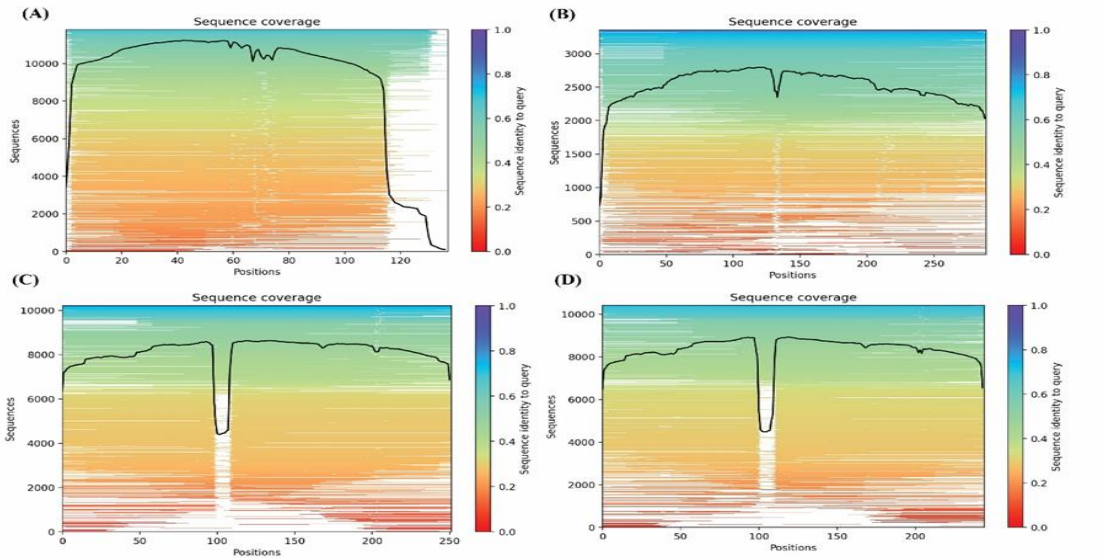

Fig. 10. Multiple sequence alignment (MSA) coverage of the four proteins, ArsC (A), ArsB (B), Acr3(1) (C), and Acr3(2) (D).

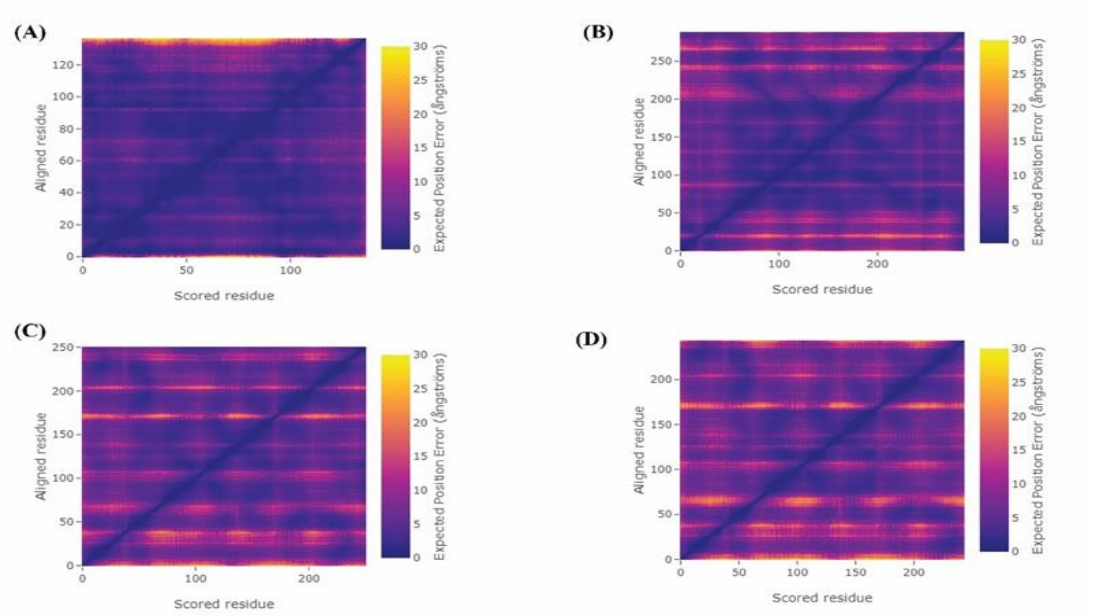

Fig. 11. Predicted Aligned Error (PAE) of the four proteins (ArsC (A), ArsB (B), Acr3(1) (C) and Acr3 2) (D).

Comparative Flexibility Modeling

Protein flexibility modeling offers insights into the fluctuations of amino acid residues within a specific time frame. Each refined protein model was analyzed utilizing default parameters as provided in Fig. (12). ArsC exhibited comparatively higher fluctuations than ArsB, Acr3(1) and Acr3(2). Significantly higher fluctuations in ArsC were measured in residues 62, 72 and 132 (4.5 Å). Acr3(1) came at the second rank of fluctuations measured in residues between 102 and 122 (3.5 Å). Acr3(2) and ArsB have the same RMSD value of 3.0 in residues A102 and A216, respectively.

Protein flexibility is a critical feature in understanding how proteins undergo conformational changes over time, especially in response to environmental factors, substrate binding, or other molecular interaction (Spyrakis *et al.*, 2011). Flexibility modeling allows researchers to predict the dynamic behavior of residues, providing insights into the potential functional roles of these flexible regions (Dobbins *et al.*, 2008). Our results revealed higher fluctuations with the ArsC model. The large fluctuations might reflect conformational changes associated with ArsC's detoxification mechanism, as flexibility can facilitate binding of As substrates and the subsequent conformational transitions required for reduction and export (Rosen *et al.*, 2020). Then Acr3(1) followed ArsC in the fluctuations. Acr3(1) is an As O3 efflux pump; flexibility in this region might be key for allowing the structural rearrangements necessary for the transport of As across the membrane. Flexibility in this region could also help in substrate specificity or in transitions between different states of the transporter during the efflux cycle (Ordoñez *et al.*, 2015). Acr3(2) and ArsB are similar RMSD values. Both Acr3(2) and ArsB are involved in As detoxification, but the fact that their fluctuations are lower compared to ArsC and Acr3(1) may imply that these proteins are more structurally stable in certain functional regions, possibly relying on more rigid, consistent mechanisms for substrate handling or transport. This stability could also ensure the robustness of these proteins' roles in maintaining homeostasis during detoxification processes (Cai *et al.*, 2009).

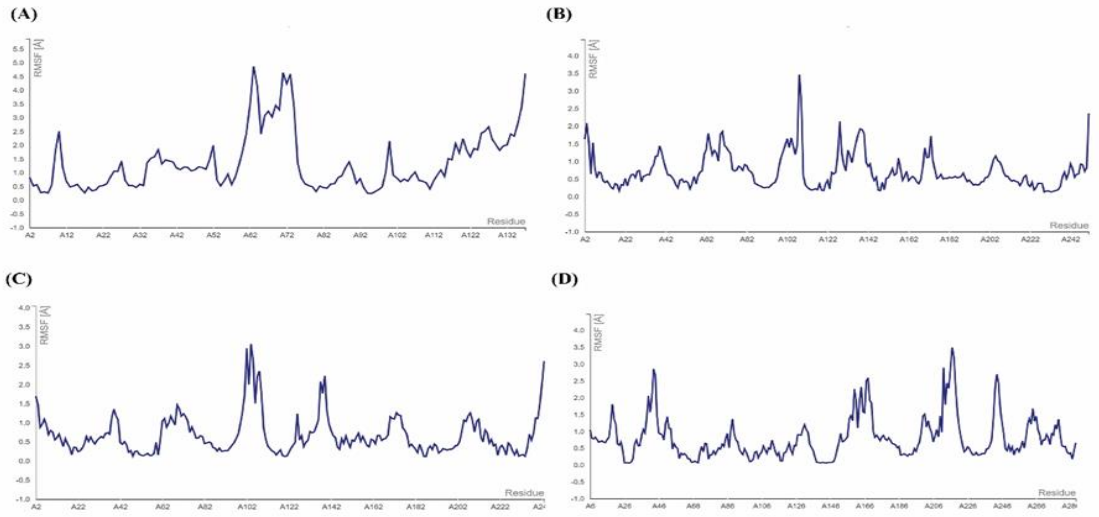

Fig. 12. Protein flexibility modeling. Protein models with a residue fluctuation plot (ArsC (A), ArsB (B), Acr3(1) (C) and Acr3(2) (D).

Molecular docking

Docking simulations were performed on the prepared proteins ArsC, ArsB, Acr3(1), and Acr3(2) utilizing As model compounds with two ligands, ART and AST. These simulations yielded accurate binding affinities and optimal conformations for each protein-ligand complex. Significant differences were observed in binding energy scores and interaction types of the docked complexes, depending on the specific residues involved. The ArsC+ART complex exhibited the strongest binding affinity with score of -2.7 kcal/mol, while ArsC+AST complex had a lower affinity of -1.1 kcal/mol, as shown in Fig. (13).

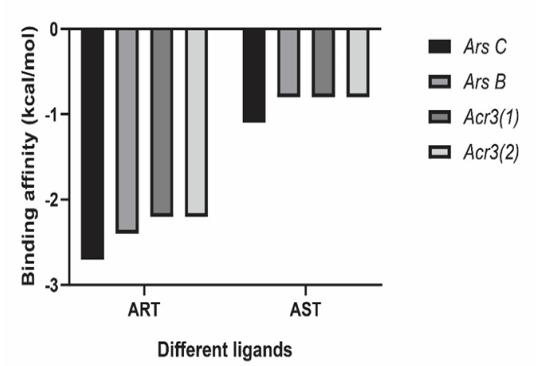

Fig. 13. Analyzing docked complexes with varying binding affinities.

Discussion

US Agency lists more than 20 HMs with high toxicity for ATSDR, but four (arsenic, lead, cadmium, and mercury) are especially harmful to human health. As the most frequent cause of acute HM poisoning among these four, As is rated first on ATSDR's "top 20 list" (Gonzalez Henao and Ghneim-Herrera 2021). Therefore, As is the main target in this work among different HMs. The collected samples from the two different industrial zones had high As concentrations that was higher than the permitted concentration limit (US EPA, 2022). Using bacteria to remove these metals from water sources is considered an eco-friendly approach (Viti *et al.*, 2014). Thirty bacterial isolates were screened as arsenic-resistant isolates and determined by their MIC and MTC to be 11500 and 9500 ppm, respectively; hence, the number of As-resistant isolates reached sixteen isolates. This was an indicator of their ability to resist high levels of As. This might be because the soil samples and industrial wastewater that were gathered were highly contaminated with high levels of various heavy metals (Elarabi *et al.*, 2023). Furthermore, The cumulative mechanistic mechanisms of stress management in bacterial bioremediation include morphological alterations, metallothionein synthesis, and siderophores production, extracellular polymeric substances, outside the cell for bacterial defense mechanisms to withstand metal toxicity and metal toxicity and facilitate environmental adaptation (Mathivanan *et al.*, 2021). The stress brought on by HM pollution can alter the traits of bacterial communities (Lin *et al.*, 2016). Sensitive soil bacteria may become less diverse and abundant, but resistant bacteria may readily adapt and become more prevalent, creating a particular bacterial community structure (Kavamura *et al.*, 2010). Bacterial activity and biomass are continuously impacted by HM pollution (Liu *et al.*, 2020). This was higher than *Bacillus cereus* and *Lysinibacillus boronitolerans*, which were resistant to As up to 3000 ppm of As O3 and As O4 with efficiency of 69.38% - 71.88% As O3 and 82.39% - 85.72%, respectively (Aguilar *et al.*, 2020). As well, this was agreed with notable studies, i.e., tolerated As concentrations of some bacterial species ranged from 150 ppm to 2585 mg/L for As O3 and 375 mg/L to 29,968 mg/L for As O34 (William and Magpantay 2023).

Before evaluation of the ability of the sixteen isolates to resist and remove As, we studied the genetic diversity between these isolates through rep-PCR DNA profiling and calculating polymorphism (%), PIC, MI, and D. Rep-PCR profiling method as a reliable tool for distinguishing closely related bacterial isolates based on DNA polymorphisms (Sharma *et al.*, 2020). These results indicate significant genetic diversity among the isolates, based on several key factors. Polymorphism is essential in differentiating between strains because it highlights variations in their DNA sequences, suggesting that the 16 isolates are genetically diverse (Brumlik *et al.*, 2004). Moreover, the clustering of isolates based on Dice similarity values highlights relationships between the isolates, with more genetically similar isolates grouped together. The heatmap helps visualize the similarities and differences, reinforcing the idea that there are distinct genetic clusters within the 16 isolates. The combination of 100% polymorphic amplicon, moderate PIC values, and high DP suggests that the 16 isolates were genetically distinct from one another.

The cell viability under As stress was evaluated and chosen for the isolates whose bacterial survival was more than 50%. Nine isolates were selected based on the highest bacterial survival under As stress for the further experiments. This was because cellular viability was most significantly impacted by greater HM concentrations, whereas lower concentrations had a less effect. One of the most frequent reasons why bacterial cell viability declines is the lack of bacterial cell respiration. Cell viability has decreased because of respiratory suppression brought on by HMs' interaction with elements of the bacterial plasma membrane (Syed *et al.*, 2021). Then, evaluation of As biosorption and its efficiency for each isolate was performed. Ars 9 isolate had the highest significant As biosorption (1415 mg/g) with efficiency (85.5%). If the toxic stress was not lethal, it could increase cell membrane permeability, leading to increased uptake of toxic ions (Odokuma and Akponah 2010). As well, nine isolates were molecularly identified into different genera and species. All these species were reported as good HM-resistant bacteria (Halema *et al.*, 2024), especially Enterobacter cloacae as a highly As-resistant bacteria (Abdelhadi *et al.*, 2024). This supports our findings.

Moreover, the adsorption of As onto the cell wall was observed through TEM images, and the difference in cellular morphology between the control and treated groups revealed the decrease in cell size in the treated group. This agreed with the study of Pagnucco *et al.*, (2023). The observed changes in cell surface morphology, such as the appearance of surface features, likely resulted from the interaction between the cells and the adsorbed metals (Pagnucco *et al.*, 2023). These alterations may be attributed to the toxic effects of the metals on the cell surface structure. Biosorption, a process that exploits the functional groups present in cell wall or extracellular metabolites, is a key mechanism for metal uptake by microorganisms. This process involves various mechanisms, including precipitation, complexation, chelation, reduction and ion exchange (Sreedevi *et al.*, 2022;

Priya *et al.*, 2022). Additionally, metal ions can disrupt cellular ion balance by attaching to the cell surface and entering the cell through ion channels or transmembrane carriers (Chen *et al.*, 2014). We can conclude that these adaptations help bacteria conserve resources and minimize the exposed surface area, thereby reducing the potential for further metal ion intrusion. The impact of ion imbalance on cell morphology, including cell size reduction, is well documented in studies using TEM to observe these ultrastructural changes under metal stress.

Enterobacter cloacae subsp. *cloacae* strain FACU1 (Ars 9) was chosen to amplify four genes closely related to As resistance, *ArsC*, *ArsB*, *Acr3(1)*, and *Acr3(2)*, purified, sequenced, and submitted into GenBank. From their deduced amino acids, the various physical and chemical parameters of the four studied proteins were computed. The 3D structure of these proteins and ligands was prepared for molecular docking. As O4 and As O3 are both the most widely encountered forms of As on a global scale owing to their toxic attributes and have negative impacts on human health (Sahu *et al.*, 2019; Fatoki *et al.*, 2022). Many bacteria have had extensive research done on the proteins linked to As reduction, including *Acidothiobacillus ferrooxidans*, *Enterobacter* sp., and *Klebsiella* sp. (Abbas *et al.* 2014; Kamde *et al.*, 2018; Ahmad *et al.*, 2023). Although computational methods have been used, the precise atomic-level molecular processes of proteins involved in the degradation of As remain poorly understood. Nevertheless, by using computational approaches wisely, these challenges may be addressed. Therefore, our study aimed to investigate the binding mechanism and chemical interactions between two model compounds, ART and AST, and four target proteins.

Homology modeling obtained a protein model employing SWISS-MODEL and AlphaFold 2. The assessment of the 3D protein structure models was carried out. Homology modeling is a powerful method to predict protein structures when an experimentally determined structure is unavailable. SWISS-MODEL and AlphaFold 2 are widely used for such purposes (Kumar and Sharma 2023). Both tools provide several metrics to evaluate the quality of the models. For a model to be considered good, GMQE should be above 0.6 (Waterhouse *et al.*, 2018), MolProbity Score should be under 2.0 (the lower, the better) (Chen *et al.*, 2012), Ramachandran Favored should be above 90%, and Ramachandran Outliers should be minimal (less than 1%) (Gopalakrishnan *et al.*, 2007), Rotamer Outliers, Bad Bonds, and Bad Angles should be close to zero (Hintze *et al.*, 2016), pLDDT values should generally be higher than 70, with high-confidence regions showing values above 90 (Carugo 2023), MSA Coverage should be broad enough to cover critical regions (Bryant and Noé 2024), and PAE values should show minimal error (darker colors on the plot, indicating lower uncertainty) (Agarwal and McShan 2024). Hence, all these parameters obtained in the four protein models suggest good structural confidence and high quality and certainty.

Molecular docking is a reliable computational method utilized to predict protein-ligand interactions and their binding affinities. It is commonly employed to identify optimal binding conformations and understand the underlying mechanisms of biomolecular interactions, including those involved in heavy metal bioremediation (Waszkowycz *et al.*, 2011; Akter *et al.*, 2017; Banerjee *et al.*, 2022; Ahmad *et al.*, 2024). This study employed molecular docking simulations to explore the binding interactions between four potential arsenic-resistant proteins (ArsC, ArsB, Acr3(1), and Acr3(2)) and two arsenic model compounds (ART and AST). The results revealed significant differences in binding affinities and interaction patterns between the protein-ligand complexes. The ArsC+ART complex exhibited the strongest binding affinity with a score of -2.7 kcal/mol, while the ArsC+AST complex had a lower affinity of -1.1 kcal/mol. This was agreed with the previous study of Ahmad *et al.*, (2024). So, the binding affinity of proteins complex with ART was higher than with AST. The reasons behind these findings may be because ArsC specifically catalyzes the reduction of As O4 to As O3 (Martin *et al.*, 2001). ArsC is evolutionarily optimized to bind As O4 due to its specific catalytic role in reducing As O4 to As O3. The enzyme's active site is structured to accommodate the tetrahedral geometry of arsenate. As O3, in contrast, is a neutral trivalent form (As O3) and does not fit into the same binding site as effectively as arsenate, which is negatively charged and tetrahedral (Bhati *et al.*, 2023). In addition, ArsB is involved in pumping As O3 out of the cell, especially when paired with ArsA, an ATPase that energizes the transport process (Garbinski *et al.*, 2019). Additionally, Acr3 is another As O3-specific transporter that helps remove As O3 from the cytoplasm (Galván *et al.*, 2021). After ArsC reduces As O4 to As O3, the enzyme will naturally be exposed to As O3. However, ArsC's affinity for As O3 was generally lower than its affinity for arsenate. Once As O4 is reduced to As O3, the enzyme does not need to bind tightly to As O3. Instead, As O3 is released from the enzyme so that it can be exported from the cell via efflux pumps (e.g., ArsB or Acr3) (Udema 2023). Transporter proteins, especially those involved in detoxification (like ArsB and Acr3), do not need high binding affinity. Instead, they require balance between the binding affinity and release efficiency. That allows them to grab the substrate, transport it, and release it quickly for efficient operation (De Wolf *et al.*, 2000). This information supports our findings.

In conclusion, the bacteria isolated from industrial zones often exhibit high resistance to HMs due to prolonged exposure to contaminated environments. In these zones, HMs may be present in toxic concentrations. This consistent exposure exerts selective pressure, favoring bacteria with robust resistance mechanisms. Molecular docking plays a crucial role in understanding HM resistance in bacteria by providing insights into the interactions between bacterial proteins and HM ions at an atomic level. Moreover, it provides a detailed understanding of the protein-ligand interactions critical to bacterial metal resistance, aiding in the design of effective strategies for bioremediation and environmental management.

Funding

No funds, grants, or other support was received.

Data availability

Data will be made available on request.

Declarations

Competing interests

The authors declare no competing interests.

REFERENCES

Abbas, S.Z., Riaz, M., Ramzan, N., Zahid, M.T., Shakoori, F.R., Rafatullah, M. (2014). Isolation and characterization of arsenic resistant bacteria from wastewater. Braz. J. Microbiol. 45(4), 1309–15. https://doi.org/10.1590/S1517-83822014000400022.

Abdelhadi, A.A., Elarabi, N.I., Ibrahim, S.M., Abdel-Maksoud, M.A., Abdelhaleem, H.A.R., Almutairi, S., Malik, A., Kiani, B.H., Henawy, A.R., Halema, A.A. (2024). Hybrid-genome sequence analysis of Enterobacter cloacae FACU and morphological characterization: insights into a highly arsenic-resistant strain. Funct. Integr. Genomics, 24(5), 1-20. https://doi.org/10.1007/s10142-024-01441-9.

Abdelhadi, A.A., Elarabi, N.I., Salim, R.G., Sharaf, A.N., Abosereh, N.A. (2016). Identification, characterization and genetic improvement of bacteriocin producing lactic acid bacteria. Biotechnology 15(3/4), 76-85. https://doi.org/10.3923/biotech.2016.76.85.

Achour, A.R., Bauda, P., Billard, P. (2007). Diversity of arsenite transporter genes from arsenic-resistant soil bacteria. Res. microbial. 158(2), 128-137. https://doi.org/ 10.1016/j.resmic.2006.11.006.

Afzal, A.M., Rasool, M.H., Waseem, M., Aslam, B. (2017). Assessment of heavy metal tolerance and biosorptive potential of Klebsiella variicola isolated from industrial effluents. AMB Express 7(1), 184. https://doi.org/10.1186/s13568-017-0482-2.

Agarwal, V., McShan, A.C. (2024). The power and pitfalls of AlphaFold2 for structure prediction beyond rigid globular proteins. Nat. Chem. Biol. 20(8), 950-959. https://doi.org/10.1038/s41589-024-01638-w.

Aguilar, N.C., Faria, M.C.S., Pedron, T., Batista, B.L., Mesquita, J.P., Bomfeti, C.A., Rodrigues, J.L. (2020). Isolation and characterization of bacteria from a brazilian gold mining area with a capacity of arsenic bioaccumulation. Chemosphere 240, 124871. https://doi.org/10.1016/j.chemosphere.2019.124871.

Ahmad, I., Singh, A.K., Katari, S.K. (2023). In silico insight into structural and functional attributes of arsenic resistance proteins from Rhizobium radiobacter strain F4J. Hazard Mater. Adv. 12, 100329. https://doi.org/10.1016/j.hazadv.2023.100329.

Ahmed, I., Singh, A.K., Mohd, S., Katari, S.K., Nalamolu, R.M., Ahmad, A., Baothman, O.A., Hosawi, S.A., Altayeb, H., Nadeem, M.S., Ahmad, V. (2024). In silico insights into the arsenic binding mechanism deploying application of computational biology-based toolsets. ACS omega, 9(7), 7529-7544. https://doi.org/ 10.1021/acsomega.3c06313.

Akhter, M., Tasleem, M., Alam, M.M., Ali, S. (2017). In silico approach for bioremediation of arsenic by structure prediction and docking studies of arsenite oxidase from Pseudomonas stutzeri TS44. Int. Biodeterior. Biodegradation 122, 82-91. https:// doi. org/10 .1016/j.ibiod.2017.04.021.

Aljohani, F.S., Abu-Dief, A.M., El-Khatib, R.M., Al-Abdulkarim, H.A., Alharbi, A., Mahran, A., Khalifa, M.E., El-Metwaly, N.M. (2021). Structural inspection for novel Pd (II), VO(II), Zn (II) and Cr (III)-azomethine metal chelates: DNA interaction, biological screening and theoretical treatments. J. Mol. Struct. 1246, 131139. https:// doi. org/ 10.10 16/j.molstruc.2021.131139.

Amiryousefi, A., Hyvönen, J., Poczai, P. (2018). iMEC: Online marker efficiency calculator. Appl. Plant Sci. 6(6), e01159. https://doi.org/ 10.1002/aps3.1159.

Azimi, R., Ozgul, M., Kenney, M. C., Kuppermann, B.D. (2024). Bioinformatic analysis of small humanin like peptides using AlfaFold-2 and Expasy ProtParam. Invest. Ophthalmol. Vis. Sci. 65(7), 1320-1320.

Banerjee, P., Chatterjee, A., Jha, S., Bhadani, N.K., Datta, P.P., Sengupta, T.K. (2022). Biochemical, molecular and in silico characterization of arsenate reductase from Bacillus thuringiensis KPWP1 tolerant to salt, arsenic and a wide range of pH. Arch. Microbiol. 204(1), 46. https://doi.org/ 10.1007/s00203-021-02660-5.

Banerjee, S., Datta, S., Chattyopadhyay, D., Sarkar, P. (2011). Arsenic accumulating and transforming bacteria isolated from contaminated soil for potential use in bioremediation. J. Environ. Sci. Health A Tox. Hazard. Subst. Environ. Eng. 46(14), 1736–1747. https://doi.org/ 10.1080/10934529.2011.623995.

Berman, H.M., Westbrook, J., Feng, Z., Gilliland, G., Bhat, T.N., Weissig, H., Shindyalov, I.N., Bourne, P.E. (2000). The Protein Data Bank. Nucleic Acids Res. 2000, 28 (1), 235–242. https://doi.org/10.1093/nar/28.1.235.

Bhati, R., Nigam, A., Ahmad, S., Raza, K., Singh, R. (2023). Structural–functional analysis and molecular characterization of arsenate reductase from Enterobacter cloacae RSC3 for arsenic biotransformation. 3 Biotech, 13(9), 305. https://doi.org/ 10.1007/s13205-023-03730-9.

Botes, E., Van Heerden, E., Litthauer, D. (2007). Hyper-resistance to arsenic in bacterial isolated from an antimony mine in South Africa. S. Afr. J. Sci. 103(7-8), 279–281. https://hdl.handle.net/10520/EJC96703

Brumlik, M.J., Bielawska-Drozd, A., Zakowska, D., Liang, X., Spalletta, R.A., Patra, G., Delvecchio, V.G. (2004). Genetic diversity among Bacillus anthracis, *Bacillus cereus* and *Bacillus thuringiensis* strains using repetitive element polymorphism-PCR. Pol. J. Microbiol. 53(4), 215-225.

Bryant, P., & Noé, F. (2024). Improved protein complex prediction with AlphaFold-multimer by denoising the MSA profile. PLoS Comput. Biol. 20(7), e1012253. https://doi.org/10.1371/journal.pcbi.1012253.

Burghardt, R.C., Droleskey, R. (2006). Transmission electron microscopy. Curr. Protoc. Microbiol. Chapter 2:Unit 2B.1. https:/ /doi.org /10.10 02/9780 4717 29 25 9.mc02b01s03.

Cai, L., Liu, G., Rensing, C., Wang, G. (2009). Genes involved in arsenic transformation and resistance associated with different levels of arsenic-contaminated soils. BMC microbial. 9, 4. https://doi.org/10.1186/1471-2180-9-4.

Capella-Gutiérrez, S., Silla-Martínez, J.M., Gabaldón, T. (2009). trimAl: a tool for automated alignment trimming in large-scale phylogenetic analyses. Bioinformatics 25(15), 1972-1973. https:// doi.o rg/10.1093 /bioinformatics/btp348.

Carugo, O. (2023). pLDDT Values in AlphaFold2 Protein Models Are Unrelated to Globular Protein Local Flexibility. Crystals 13(11), 1560. https://doi.org/ 10.3390/cryst13111560.

Castro-Severyn, J., Pardo-Esté, C., Mendez, K.N., Fortt, J., Marquez, S., Molina, F., Castro-Nallar, E., Remonsellez, F., Saavedra, C.P. (2021). Living to the high extreme: unraveling the composition, structure, and functional insights of bacterial communities thriving in the arsenic-rich Salar de Huasco altiplanic ecosystem. Microbiol. Spectr. 9(1), e0044421. https://doi.org/10.1128/Spectrum.00444-21.

Çepni, E., Gürel, F. (2012). Variation in extragenic repetitive DNA sequences in Pseudomonas syringae and potential use of modified REP primers in the identification of closely related isolates. Genet. Mol. Biol. 35(3), 650-656. https://doi.org/ 10.1590/S1415-47572012005000040.

Chen, J.L., Ortiz, R., Steel, T.W.J., Stuckey, D.C. (2014). Toxicants inhibiting anaerobic digestion: a review. Biotechnol. Adv. 32(8), 1523-1534. https://doi.org/ 10.1016/j.biotechadv.2014.10.005.

Chen, V.B., Arendall, W.B. 3rd, Headd, J.J., Keedy, D.A., Immormino, R.M., Kapral, G.J., Murray, L.W., Richardson, J.S., Richardson, D.C. (2010). MolProbity: all-atom structure validation for macromolecular crystallography. Acta Crystallogr. D Biol. Crystallogr. 66(1), 12-21. https://doi.org/ 10.1107/S0907444909042073.

Chowdhury, R., Sen, A.K., Karak, P., Chatterjee, R., Giri, A.K., Chaudhuri, K. (2009). Isolation and characterization of an arsenic-resistant bacterium from a bore-well in West Bengal, India. Ann. Microbiol. 59, 253–258. https://doi.org/10.1007/BF03178325

Cui, J., Jing, C.A. (2019). A review of arsenic interfacial geochemistry in groundwater and the role of organic matter. Ecotoxicol. Environ. Saf. 183, 109550. https://doi.org/10.1016/j.ecoenv.2019.109550.

de Wolf, F.A., Brett, G.M. (2000). Ligand-binding proteins: their potential for application in systems for controlled delivery and uptake of ligands. Pharmacol Rev. 52(2), 207-236.

Desai, S.A., Patel, V.P., Shinde, S.U., Kadam, S.S. (2024). In silico studies for the bioremediation of heavy metals from contaminated sites. In: Parray, J.A., Li, W., (Eds.), Microbiome-assisted bioremediation: rehabilitating agricultural soils. Academic Press Inc., London, pp. 139-148.

Dey, U., Chatterjee, S., Mondal, N.K. (2016). Isolation and characterization of arsenic-resistant bacteria and possible application in bioremediation. Biotechnol. Rep. 10, 1–7. https://doi.org/10.1016/j. btre .201 6.02.002

Dobbins, S.E., Lesk, V.I., Sternberg, M.J. (2008). Insights into protein flexibility: the relationship between normal modes and conformational change upon protein–protein docking. Proc. Natl. Acad. Sci. USA, 105(30), 10390-10395. https://doi.org/10.1073/pnas.0802496105.

Dunivin, T.K., Yeh, S.Y., Shade, A. (2019). A global survey of arsenic related genes in soil microbiomes. BMC boil. 17(1), 45. https://doi.org/10.1186/s12915-019-0661-5

Eberhardt, J., Santos-Martins, D., Tillack, A.F., Forli, S. (2021). AutoDock Vina 1.2.0: New Docking Methods, Expanded Force Field, and Python Bindings. J. Chem. Inf. Model. 61(8), 3891–3898. https://doi.org/10.1021/acs.jcim.1c00203.

Elarabi, N.I., Halema, A.A., Abdelhadi, A.A., Henawy, A.R., Samir, O., Abdelhaleem, H.A. (2023). Draft genome of Raoultella planticola, a high lead resistance bacterium from industrial wastewater. AMB Express 13(1), 14. https://doi.org/ 10.1186/s13568-023-01519-w.

El-Beltagi, H.S., Halema, A.A., Almutairi, Z.M., Almutairi, H.H., Elarabi, N.I., Abdelhadi, A.A., Henawy, A.R., Abdelhaleem, H.A.R. (2024). Draft genome analysis for Enterobacter kobei, a promising lead bioremediation bacterium. Front. Bioeng. Biotechnol. 11, 1335854. https://doi.org/ 10.3389/fbioe.2023.1335854.

Fatoki, J.O., Badmus, J.A. (2022). Arsenic as an environmental and human health antagonist: A review of its toxicity and disease initiation. J. Hazard. Mater. Adv. 5, 100052. https://doi.org/10.1016/j.hazadv.2022.100052.

Finnegan, P.M., Chen, W., 2012. Arsenic toxicity: the effects on plant metabolism. Front. Physio. 3, 182. https://doi.org/10.3389/fphys.2012.00182.

Forli, S., Huey, R., Pique, M.E., Sanner, M.F., Goodsell, D.S., Olson, A.J. (2016). Computational protein–ligand docking and virtual drug screening with the AutoDock suite. Nat. Protoc. 11 (5), 905–919. https:// doi .org/ 10.1038/nprot.2016.051.

Fu, H.L., Meng, Y., Ordóñez, E., Villadangos, A.F., Bhattacharjee, H., Gil, J.A., Mateos, L.M., Rosen, B.P. (2009). Properties of arsenite efflux permeases (Acr3) from Alkaliphilus metalliredigens and Corynebacterium glutamicum. J. Biol. Chem., 284 (30) :19887-95. https:// doi.org/ 10. 1074 /jbc .M109. 011882. Epub 2009 Jun 3. PMID: 19494117; PMCID: PMC2740414.

Galván, A.E., Paul, N.P., Chen, J., Yoshinaga-Sakurai, K., Utturkar, S.M., Rosen, B.P., Yoshinaga, M. (2021). Identification of the biosynthetic gene cluster for the organoarsenical antibiotic arsinothricin. Microbiol. Spectr. 9(1), e0050221. https://doi.org/ 10.1128/Spectrum.00502-21.

Garbinski, L.D., Rosen, B.P., Chen, J. (2019). Pathways of arsenic uptake and efflux. Environ. Int. 126, 585–597. https://doi.org/10.1016/j.envint.2019.02.058.

Genersch, E., Otten, C. (2003). The use of repetitive element PCR fingerprinting (rep-PCR) for genetic subtyping of German field isolates of Paenibacillus larvae subsp. larvae. Apidologie, 34(3), 195-206. https://doi.org/10.1051/apido:2003025.

Gevers, D., Huys, G., Swings, J. (2001). Applicability of rep-PCR fingerprinting for identification of Lactobacillus species. FEMS microbiol. lett. 205(1), 31-36. https://doi.org/ 10.1111/j.1574-6968.2001.tb10921.x.

Gonzalez Henao, S., Ghneim-Herrera, T. (2021). Heavy metals in soils and the remediation potential of bacteria associated with the plant microbiome. Front. Environ. Sci. 9, 604216. https:// doi .org /10. 3389 /fenvs.2021.604216.

Gopalakrishnan, K., Sowmiya, G., Sheik, S.S., Sekar, K. (2007). Ramachandran plot on the web (2.0). Protein Pept Lett. 14(7), 669-671. https:/ /doi .org/1 0.2174 /092986607781483912.

Halema, A.A., Abdel-Maksoud, M.A., Ali, M.Y., Abdul Malik, Kiani, B.H., Henawy, A.R., Elarabi, N.I., Abdelhadi, A.A., Abdelhaleem, H.A.R. (2024). New complete genome insights into Enterobacter roggenkampii FACU2: a potential player in cadmium bio-removal. World J. Microbiol. Biotechnol., 18,41(1):2. https://doi.org/10.1007/s11274-024-04138-0

Halema, A.A., El-Beltagi, H.S., Al-Dossary, O., Alsubaie, B., Henawy, A.R., Rezk, A.A., Almutairi, H.H., Mohamed, A.A., Elarabi, N.I., Abdelhadi, A.A. (2024). Omics technology draws a comprehensive heavy metal resistance strategy in bacteria. World J. Microbiol. Biotechnol. 40, 193. https://doi.org/10.1007/s11274-024-04005-y

Henawy, A.R., Abdelhadi, A.A., Halema, A.A., Refae, R.I., Barakat, O.S. (2023). Exopolysaccharide production from agro-industrial wastes by lactic acid bacteria isolated from silage. Egypt. Pharm. J., 22(3), 403-414. https://doi.org/10.4103/epj.epj_63_23

Hintze, B.J., Lewis, S.M., Richardson, J.S., Richardson, D.C. (2016). Molprobity's ultimate rotamer-library distributions for model validation. Proteins, 84(9), 1177-1189. https://doi.org/10.1002/prot.25039

Jamroz, M., Kolinski, A., Kmiecik, S. (2013). CABS-flex: server for fast simulation of protein structure fluctuations. Nucleic Acids Res., 41 (W1), W427–W431. https://doi.org/10.1093/nar/gkt332.

Kamde, K., Pandey, R.A., Thul, S., Bansiwal, A. (2018). Removal of arsenic by Acidothiobacillus ferrooxidans bacteria in bench scale fixed-bed bioreactor system. Chem. Ecol., 34 (9), 818–838. https:// doi.org /10.1080/02757540.2018.1504927.

Kavamura, V.N., Esposito, E. (2010). Biotechnological strategies applied to the decontamination of soils polluted with heavy metals. Biotechnol. Adv., 28, 61–69. https://doi.org/10.1016/j.biotechadv.2009.09.002

Khan, A.H., Rasul, S.B., Munir, A., Habibuddowla, M., Alauddin, M., Newaz, S.S., Hussan, A. (2000). Appraisal of a simple arsenic removal method for groundwater of Bangladesh, J. Environ. Sci. Health, 35, 1021–1041. https:// doi. org/ 10.10 80/10934520009377018

Kruger, M.C., Bertin, P.N., Heipieper, H.J., Arsène-Ploetze, F. (2013). Bacterial metabolism of environmental arsenic--mechanisms and biotechnological applications. Appl. Microbiol. Biotechnol., 97, 3827–3841. https://doi.org/10.1007/s00253-013-4838-5

Kumar, R., Sharma, A. (2023). Computational strategies and tools for protein tertiary structure prediction, in Bhatt, A.K., Bhatia, R.K., Bhalla, T.C. (Eds.), Basic biotechniques for bioprocess and bioentrepreneurship. Academic Press, United kingdom pp. 225-242. https://doi.org/10.1016/B978-0-12-816109-8.00015-5.

Lin, W., Huang, Z., Li, X., Liu, M., Cheng, Y. (2016). Bio-remediation of acephate-Pb (II. compound contaminants by Bacillus subtilis FZUL-33). J. Environ. Sci.,45, 94–99. https://doi.org/10.1016/j.jes.2015.12.010

Liu, H., Wang, C., Xie, Y., Luo, Y., Sheng, M., Xu, F., Xu, H. (2020). Ecological responses of soil microbial abundance and diversity to cadmium and soil properties in farmland around an enterprise-intensive region. J. Hazard. Mater., 392, 122478. https: //doi .org/10.1016/j.jhazmat.2020.122478

Lopez-Maury, L., Florencio, F.J., Reyes, J.C. (2003). Arsenic sensing and resistance system in the cyanobacterium Synechocystis sp. strain PCC 6803. J. Bacteriol., 185, 5363e5371. https://doi.org/10.1128/JB.185.18.5363-5371.2003

Lou, L.Q., Ye, Z.H., Wong, M.H. (2009). A comparison of arsenic tolerance, uptake and accumulation between arsenic hyperaccumulator, Pteris vittata L. and non-accumulator, P. semipinnata L.-A hydroponic study. J. Hazard. Mater., 171 (1–3), 436–442. https:// doi. org/1 0.1016/j.jhazmat.2009.06.020

Madeira, F., Park, Y.M., Lee, J., Buso, N., Gur, T., Madhusoodanan, N., Basutkar, P., Tivey, A.R., Potter, S.C., Finn, R.D., Lopez, R. (2019). The EMBL-EBI search and sequence analysis tools APIs in 2019. Nucleic Acids Res., 2, 47(W1):W636-41. https://doi.org/10.1093/nar/gkz268

Malik, A., Jaiswal, R. (2000). Metal resistance in Pseudomonas strains isolated from soil treated with industrial wastewater. World J. Microbiol. Biotechnol., 16, 177–182. https:// doi.org/1 0.1023/ A:1008905902282

Mandal, B.K., Suzuki, K.T. (2002). Arsenic around the world: a review, Talanta 58, 201–235. https: //doi.or g/10.1016/S0039-9140(02)00268-0

Martin, P., DeMel, S., Shi, J., Gladysheva, T., Gatti, D. L., Rosen, B. P., Edwards, B.F. (2001). Insights into the structure, solvation, and mechanism of ArsC arsenate reductase, a novel arsenic detoxification enzyme. Structure, 9(11), 1071-1081. https:// doi. org/ 10.1 016/s0969-2126(01)00672-4

Mathivanan, K., Chandirika, J.U., Vinothkanna, A., Yin, H., Liu, X., Meng, D. (2021). Bacterial adaptive strategies to cope with metal toxicity in the contaminated environment–A review. Ecotoxicol. Environ. Saf., 226, 112863. https:/ /doi. org/1 0.101 6/j.e coenv .2021.112863

Mendiburu, F., Yaseen, M. (2020). agricolae: Statistical Procedures for Agricultural Research. R package version 1.4. 0 , https:/ /myas een20 8.github .io/agricolae/https://cran.r-project.org/package=agricolae.

Meng, Y.L., Liu, Z., Rosen, B.P. (2004). As(III) and Sb(III) uptake by GlpF and efflux by ArsB in Escherichia coli. J. Biol. Chem., 279,18334e18341. https://doi.org/10.1074/jbc.M400037200

Morris, G.M., Huey, R., Lindstrom, W., Sanner, M.F., Belew, R.K., Goodsell, D.S., Olson, A.J. (2009). AutoDock4 and AutoDockTools4: Automated docking with selective receptor flexibility. J. Comput. Chem., 30 (16), 2785–2791. https://doi.org/10.1002/jcc.21256.

Mukhopadhyay, R., Rosen, B.P., Phung, L.T., Silver, S. (2002). Microbial arsenic: from geocycles to genes and enzymes. FEMS Microbiol. Rev., 26:311–325. https://doi.org/10.1111/j.1574-6976. 2002.tb00617.x

Odokuma, L.O., Akponah, E. (2010). Effect of concentration and contact time on heavy metal uptake by three bacterial isolates. J. Environ. Chem. Ecotoxicol, 2(6), 84-97.

Ordonez, E., Letek, M., Valbuena, N., Gil, J.A., Mateos, L.M. (2005). Analysis of genes involved in arsenic resistance in *Corynebacterium glutamicum* ATCC 13032. Appl. Environ. Microbiol., 71, 6206e6215. https://doi.org/10.1128/AEM.71.10.6206-6215.2005

Ordoñez, O.F., Lanzarotti, E., Kurth, D., Cortez, N., Farías, M.E., Turjanski, A.G. (2015). Genome comparison of two Exiguobacterium strains from high altitude andean lakes with different arsenic resistance: identification and 3D modeling of the Acr3 efflux pump. Front. environ. sci., 3, 50. https://doi.org/10.3389/fenvs.2015.00050

Pagnucco, G., Overfield, D., Chamlee, Y., Shuler, C., Kassem, A., Opara S, Tiquia-Arashiro, S.M. (2023). Metal tolerance and biosorption capacities of bacterial strains isolated from an urban watershed. Front. Microbiol., 14:1278886. https:// doi. org/ 10. 3389/ fmicb. 2023.1278886

Priya, A.K., Gnanasekaran, L., Dutta, K., Rajendran, S., Balakrishnan, D., Soto-Moscoso, M. (2022). Biosorption of heavy metals by microorganisms: evaluation of different underlying mechanisms. Chemosphere, 307,135957. https:// doi. org/10.1016/j.chemosphere.2022.135957

Rosen, B.P. (2002). Biochemistry of arsenic detoxification. FEBS Lett., 529, 86e92. https://doi. org/10.1016/s0014-5793(02)03186-1

Rosen, M. R., Leuthaeuser, J.B., Parish, C.A., Fetrow, J.S. (2020). Isofunctional clustering and conformational analysis of the arsenate reductase superfamily reveals nine distinct clusters. Biochem., 59(44), 4262-4284. https://doi. org/10.1021/acs.biochem.0c00651

Sahu, S., Sheet, T., Banerjee, R. (2019). Interaction landscape of a 'CαNN' motif with arsenate and arsenite: a potential peptide-based scavenger of arsenic. RSC Adv., 9 (2), 1062–1074. https://doi. org/10.1039/C8RA08225A.

Sato, T., Kobayashi, Y. (1998). The ars operon in the skin element of Bacillus subtilis confers resistance to arsenate and arsenite. J. Bacteriol., 180, https://doi. org/1655e1661. 10.1128/jb.180.7.1655-1661.1998

Schwede, T., Kopp, J., Guex, N., Peitsch, M.C. (2003). SWISS-MODEL: an automated protein homology-modeling server. Nucleic acids res., 31(13), 3381-3385. https://doi. org/10.1093/nar/gkg520

Selvi, M.S., Sasikumar, S., Gomathi, S., Rajkumar, P., Sasikumar P., Sadasivam, S.G. (2014). Isolation and characterization of arsenic resistant bacteria from agricultural soil, and their potential for arsenic bioremediation. I.J.A.P.R., 2 (11), 393-405. http://dx.doi.org/10.15739/IJAPR.012

Shakoori, F.R., Aziz, I., Rehman, A., Shakoori, A. (2010). Isolation and characterization of arsenic reducing bacteria from industrial effluents and their potential use in bioremediation of wastewater. Pak. J. Zool., 42,331-338.

Shankar, S., Shanker, U., Shikha (2014). Arsenic contamination of groundwater: a review of sources, prevalence, health risks, and strategies for mitigation. Scientific World Journal 2014, 304524. https:// doi. org/ 10.1155/2014/304524.

Sharma, A., Lee, S., Park, Y.S. (2020). Molecular typing tools for identifying and characterizing lactic acid bacteria: a review. Food science and biotechnol., 29, 1301-1318. https://doi.org/10.1007/s10068-020-00802-x

Shi, K., Li, C., Rensing, C., Dai, X., Fan, X., Wang, G. (2018). Efflux transporter ArsK is responsible for bacterial resistance to arsenite, antimonite, trivalent roxarsone, and methylarsenite. Appl. Environ. Microbiol., 84, e01842–e01818. https: //doi .org/ 10.1128/AEM.01842-18

Shivaji, S., Suresh, K., Chaturvedi, P., Dube, S., Sengupta, S. (2005). *Bacillus arsenicus* sp. nov., an arsenic-resistant bacterium isolated from a siderite concretion in West Bengal, India. Int. J. Syst. Evol. Microbiol., 55, 1123–1127. https://doi.org/10.1099/ijs.0.63476-0

Shoham, S., Weinberger, A., Kaplan, A., Avisar, D., Ilan, M. (2021). Arsenate reducing bacteria isolated from the marine sponge Theonella swinhoei: Bioremediation potential. Ecotoxicol. Environ. Saf., 222, 112522. https://doi.org/10.1016/j.ecoenv.2021.112522.

Shrestha, R.A., Lama, B., Joshi, J., Sillanpaa, M. (2008). Effect of Mn(II) and Fe(II) on microbial removal of arsenic(III). Environ. Sci. Pollut. Res., 15, 303–307. https://doi.org/10.1007/s11356-008-0005-4

Skolnick, J., Gao, M., Zhou, H., Singh, S. (2021). AlphaFold 2: why it works and its implications for understanding the relationships of protein sequence, structure, and function. J. Chem. Inf. Model., 61(10), 4827-4831. https://doi.org/10.1021/acs.jcim.1c01114

Smedley, P.L., Kinniburgh, D.G. (2002). A review of the source, behaviour and distribution of arsenic in natural waters. Appl. Geochem., 17, 517–568. https://doi.org/10.1016/S0883-2927(02)00018-5

Spyrakis, F., BidonChanal, A., Barril, X., Javier Luque, F. (2011). Protein flexibility and ligand recognition: challenges for molecular modeling. Curr. Top. Med. Chem., 11(2), 192-210. https://doi.org/ 10.2174/156802611794863571

Sreedevi, P.R., Suresh, K., Jiang G. (2022). Bacterial bioremediation of heavy metals in wastewater: a review of processes and applications. J. Wat. Process Eng., 48:102884. https://doi.org/ 10.1016/j.jwpe.2022.102884

Syed, A., Zeyad, M.T., Shahid, M., Elgorban, A.M., Alkhulaifi, M.M., Ansari, I.A. (2021). Heavy metals induced modulations in growth, physiology, cellular viability, and biofilm formation of an identified bacterial isolate. ACS omega, 6(38), 25076-25088. https://doi.org/ 10.1021/acsomega.1c04396

Taran, M., Fateh, R., Rezaei, S., Gholi, M.K. (2019). Isolation of arsenic accumulating bacteria from garbage leachates for possible application in bioremediation. Iran J. Microbiol. 11:60–66. https://doi.org/10.18502/ijm.v11i1.707

Tasleem, M., Hussein, W.M., El-Sayed, A.A.A., Alrehaily, A. (2023). An in silico bioremediation study to identify essential residues of metallothionein enhancing the bioaccumulation of heavy metals in Pseudomonas aeruginosa. Microorganisms, 11(9), 2262. https://doi.org/10.3390/microorganisms11092262

Thomas, J.C.I.V., Oladeinde, A., Kieran, T.J., Finger, J.W., Bayona-Va´squez, N.J., Cartee, J.C., Glenn, T.C. (2020). Co-occurrence of antibiotic, biocide, and heavy metal resistance genes in bacteria from metal and radionuclide contaminated soils at the Savannah River Site. Microb. Biotechnol., 13,1179–1200. https://doi.org/10. 1111/1751-7915.13578

Tsai, S., Singh, S., Chen, W. (2009). Arsenic metabolism by microbes in nature and the impact on arsenic remediation. Current Opinion Biotechnol., 20, 659–667. https://doi.org/10.1016/j.copbio.2009.09.013

Udema, I.I. (2023). The life span of steps in the enzyme-catalyzed reaction, its implications, and matters of general interest. bioRxiv., 2023-01. https:// doi. org/ 10.1101/2023.01.08.523157

Versalovic, J., Schneider, M., De, Bruijn, F.J., Lupski, J.R. (1994). Genomic fingerprinting of bacteria using repetitive sequence-based polymerase chain reaction. Methods Mol Biol., 5(1):25-40.

Vijayaraghavan, K., Yun, Y.S. (2008). Bacterial biosorbents and biosorption. Biotechnol. Adv., 26(3), 266–291. https://doi.org/10.1016/j.biotechadv.2008.02.002

Viti, C., Marchi, E., Decorosi, F., Giovannetti, L. (2014). Molecular mechanisms of Cr(VI) resistance in bacteria and fungi. FEMS Microbiol. Rev., 38(4),633-59. https://doi.org/10.1111/1574-6976.12051. Epub 2013 Dec 3. PMID: 24188101

Waszkowycz, B., Clark, D.E., Gancia, E, (2011). Outstanding challenges in protein–ligand docking and structure-based virtual screening. Wiley Interdisciplinary Reviews: Comput. Mol. Sci., 1(2), 229-259. https://doi.org/10.1002/wcms.18

Waterhouse, A., Bertoni, M., Bienert, S., Studer, G., Tauriello, G., Gumienny, R., Schwede, T. (2018). SWISS-MODEL: homology modelling of protein structures and complexes. Nucleic acids res., 46(W1), W296-W303. https://doi.org/10.1093/nar/gky427. PMID: 29788355; PMCID: PMC6030848.

William, V.U., Magpantay, H.D. (2023). Arsenic and microorganisms: genes, molecular mechanisms, and recent advances in microbial arsenic bioremediation. Microorganisms, 12(1), 74. https://doi.org/10.3390/microorganisms12010074

Wysocki, R., Bobrowicz, P., Ulaszewski, S. (1997). The Saccharomyces cerevisiae ACR3 gene encodes a putative membrane protein involved in arsenite transport. J. Biol. Chem., 272, 30061e30066. https://doi.org/10.1074/jbc.272.48.30061

Wysocki, R., Clemens, S., Augustyniak, D., Golik, P., Maciaszczyk, E., Tamas, M.J., Dziadkowiec, D. (2003). Metalloid tolerance based on phytochelatins is not functionally equivalent to the arsenite transporter Acr3p, Biochem. Biophys. Res. Commun., 304 (2003) 293e300. https://doi.org/10.1016/s0006-291 x (03) 00584-9

Yang, Y., Wu, S., Lilley, R. M., Zhang, R. (2015). The diversity of membrane transporters encoded in bacterial arsenic-resistance operons. PeerJ 3:e943. https://doi.org/10.7717/peerj.943

Zemanova´, V., Pavlı´kova´, D., Hnilicˇka, F., Pavlı´k, M., 2021. Arsenic Toxicity-Induced Physiological and Metabolic Changes in the Shoots of Pteris cretica and Spinacia oleracea. Plants, 10:2009. https:/ /doi .org/ 10.3390/plants10102009

Zhu, X.H., Zhang, P.P., Chen, X.G., Wu, D.D., Ye, Y. (2016). Natural and anthropogenic influences on the arsenic geochemistry of lacustrine sediment from a typical fault-controlled high land lake: Yangzonghai Lake, Yunnan. China Environ Earth Sci., 75:217 .https: //doi. org/ 10.1007/s12665-015-4924-3

استكشاف الرؤى الجينية والبنيوية باستخدام الحاسب الالى لبروتينات المقاومة في سلالة *Enterobacter* المعالجة بالزرنيخ

أسماء أحمد حليمة[1] ، هبة عبد الحليم رضوان عبد الحليم [2]، أحمد رجب الحناوي [3]، نجوى أبراهيم العربي[1]*، عبد الهادي عبدالله عبد الهادي [1] و داليا سيد أحمد [1]

[1]قسم الوراثة، كلية الزراعة، جامعة القاهرة؛ الجيزة، 12613، مصر
[2]كلية التكنولوجيا الحيوية، جامعة مصر للعلوم والتكنولوجيا؛ مدينة 6 أكتوبر، مصر.
[3]قسم الميكروبيولوجيا الزراعية، كلية الزراعة، جامعة القاهرة، الجيزة، 12613، مصر

الملخص

يتصدر الزرنيخ (As) قائمة المواد السامة فى الوكالة الامريكية لتسجيل المواد السامة والأمراض حيث أنه أحد الأسباب الرئيسية للتسمم الشديد بالمعادن الثقيلة. فى هذه الدراسة تم الحصول على ثلاثون عزلة بكتيرية مقاومة للزرنيخ ، وتم تحديد ستة عشر عزلة منهم يمكنها تحمل ما يصل إلى 11500 جزء في المليون من الزرنيخ. وقد أوضحت نتائج الواسمات الجزيئية باستخدام الواسم rep-PCR عن تنوع كبير بين هذه السلالات المقاومة. وتم اختيار تسع عزلات ذات أعلى قدرة على تحمل الزرنيخ لمزيد من الدراسة على أساس نتائج قدرة السلالات على الأمتصاص الحيوي للزرنيخ وتم تعريفها على المستوي الجزيئي. ومن بين هذه السلالات أظهرت السلالة *Enterobacter cloacae* subsp. *cloacae* FACU 1 (Ars 9) أعلى قدرة على الأمتصاص الحيوي حيث اظهرت النتائج قدرة هذه السلالة على امتصاص 85.5٪ من الزرنيخ بما يعادل 1415 مجم / جم من الكتلة الحيوية. وبإستخدام المجهر الإلكتروني النافذ TEM مع السلالة الـ Ars9 وجد أن الزرنيخ يتجمع على سطح الخلية. واكدت النتائج أن هذه السلالة تحتوى على جينات مقاومة الزرنيخ (1)Acr3 و (2)Acr3 و ArsB و ArsC . وقد تم محاكاة نماذج تشابه تركيب البروتينات الناتجة من هذه الجينات باستخدام SWISS-MODEL وAlphaFold2 وتم تطبيق الالتحام الجزيئي لتقييم تقارب ارتباطها بالزرنيخ (AsO4) والزرنيخيت (AsO3) وأشارت النتائج إلى أن ArsC أظهر تقاربًا أعلى لـ AsO4 مما يشير إلى دوره في اختزال AsO4 كما أظهرت بروتينات النقل ArsB وAcr3 تقاربًا معتدلًا لـ AsO3 مما يسهل تدفقه الفعال داخل الخلية. وتساهم هذه النتائج فى رؤية اوضح حول آليات إزالة السموم من الزرنيخ بواسطة البكتريا كما تسلط الضوء على امكانية استخدام السلالات المقاومة للزرنيخ لتطبيقات المعالجة البيولوجية.

الكلمات الدالة: Acr3(1)، ArsB، ArsC، *Enterobacter*، الالتحام الجزيئي